

AD 607663

NAVWEPS REPORT 8202

15 OCTOBER 1964

NAVWEPS REPORT 8202

VLF SUPERDIRECTIVE ARRAY WIDEBAND COMPONENTS

E. W. SEELEY

RESEARCH DEPARTMENT

COPY	2	3	1st
HARD COPY	\$.	3.00	
MICROFICHE	\$.	0.75	

DDC
 RECEIVED
 NOV 4 1964
 DDC-IRA C



NAVAL ORDNANCE LABORATORY CORONA
 CORONA, CALIFORNIA

NAVAL ORDNANCE LABORATORY CORONA

E. B. JARMAN, CAPT., USN
Commanding Officer

F. S. ATCHISON, Ph. D.
Technical Director

FOREWORD

The work described in this report was conducted in the Electronics Division of the Research Department, Naval Ordnance Laboratory, Corona, as a part of the NOLC very-low-frequency (VLF) research program, which is jointly sponsored by this Laboratory's Foundational Research Program, WepTask R360-FR-104/211-1/R011-01-01, and the Office of Naval Research, Code 418, under P. O. 3-0012.

C. J. HUMPHREYS
Head, Research Department

ABSTRACT

If improperly designed, the loops, preamplifiers, mixers, and transmission lines tend to deteriorate the directivity of VLF superdirective arrays in which they are used. This report describes the characteristics required of these components when used experimentally in superdirective arrays. Reception patterns of these arrays and illustrations of the respective capabilities of the components are given.

INTRODUCTION

Very-low-frequency (VLF) superdirective arrays have been studied at the Naval Ordnance Laboratory, Corona, California, for the past several years (Refs. 1-5). It has become increasingly clear that, if it is desired to operate effectively over the wide bandwidth of which these arrays are theoretically capable, special attention must be given to the components of the arrays. For that reason, this report examines the characteristics of the components of practical arrays.

Experimental work on these components was performed at NOLC and at the NOLC field site in Johnson Valley, California.

LOOPS, PREAMPLIFIERS, AND TRANSFORMERS

The components of VLF superdirective arrays must be broadband to utilize the broad bandwidth of the arrays. If loop antennas are used, they must be designed to avoid self-resonance or resonance with the matching input transformer of the preamplifier used with them. These design requirements are specific for operating in the 10 to 30 kc frequency band within which sferics are normally received. Broadband loops with matching transformers and preamplifiers, and delay-line mixers have been designed for sferic reception.

For this experimental work, a loop 10 ft square was selected to obtain a signal-to-noise ratio that was adequate and still allowed operation well below resonance for broad bandwidth. In a loop, the inductive reactance increases in direct proportion to the square of the number of turns, and the effective height (or signal-receiving ability) increases linearly with the number of turns. Therefore, the loop was designed to contain the minimum number of turns that was compatible with the signal needed to exceed preamplifier noise, and to maintain tolerable physical size. Because of their importance in superdirective arrays, the null depths were increased by electrostatically shielding the loops.

A broadband transformer was designed by the Thunderbird Electronics Company, Pomona, California, to match the loop to the transistorized preamplifier. The input resistance and reactance of this transformer as functions of frequency for various load resistances are given in Figs. 1 and 2. The figures show that a wide range of impedances

can be linearly matched over the 10 to 30 kc frequency range. The transformer was used to match the input impedance (Fig. 3) of the preamplifier to the loop. The gain (Fig. 4) of the transformer and preamplifier is very flat over a wide frequency range.

Signals received from several Navy VLF stations were used to determine that a four-turn loop had the greatest effective height (Fig. 5). The loop antenna was found more effective with a single shield than with pairs. The resonant frequency of the loop-preamplifier combination was measured by exciting the loop with a small coaxial transmitting loop with constant input current, and was well above the 10 to 30 kc range (Fig. 6). The four-turn, single-shielded loop was selected for the basic element of the array and additional measurements were made on it. The far-field nulls were measured by using transmissions from the Navy VLF stations, and the null depths ranged 30 to 38 db (or more) below the main lobes. The null signals were usually below the spheric noise level and were therefore not detected.

The input impedance of the loop alone was measured and compared with the theoretical reactance; the agreement was quite good (Fig. 7). For frequencies well below resonance, the theoretical inductive reactance is

$$X_L = 4\pi^2 fDN^2 \times 10^{-7} \ln \frac{D}{d} \quad (1)$$

where f = frequency

D = diameter of the loop in meters

N = number of turns in the loop

d = diameter of the wire

The effective height of a loop is a measure of its ability to receive signals. The theoretical effective height of a matched loop is

$$H_e = \frac{\pi NA}{\lambda} \quad (2)$$

where A = area of the loop, and λ = free-space wavelength. A comparison of the measured and theoretical effective heights of the 10 ft square loop is given in Fig. 8, where the theoretical curve is for a matched loop. At the higher frequencies, the loop is not matched; at frequencies beyond 25 kc, the discrepancy between theoretical and measured values becomes progressively wider.

The effective height was measured by using the standard coaxial-loop method (Ref. 6). A coaxial transmitting loop at a given distance from the test loop immerses it in an electrical field expressed by

$$E_f = \frac{60\pi r_1^2 I}{\left[R^2 + (r_1 + r_2)^2 \right]^{3/2}} \left(1 + \frac{3}{4} k^2 + \frac{75}{128} k^4 \dots \right) \quad (3)$$

where E_f = electrical field surrounding the test loop

R = distance between transmitting and test loops

r_1 = radius of the transmitting loop

r_2 = radius of the test loop

I = current in the transmitting loop

$$k^2 = \frac{4r_1 r_2}{R^2 + (r_1 + r_2)^2}$$

The effective height is

$$H_e = \frac{V_L}{E_f} \quad (4)$$

where V_L is the terminal voltage of the loop.

The effective height of the loop-preamplifier combination was measured (Fig. 9); it was determined that the height increases linearly over the 10 to 30 kc range, but levels off beyond 80 kc. The lack of increase is partly because of the inability of the transformer to match the rapidly increasing reactance of the loop to the more slowly increasing reactance of the preamplifier. The signal level of a transmitting station received with the loop-preamplifier combination can be predicted by using Fig. 9 and Eq. 4. For example, the Navy VLF station NPG (18.6 kc) in Southern California has a field strength of approximately 2 mv/m. At this frequency, the effective height of the loop-preamplifier combination is 24 m (from Fig. 8). Therefore, from Eq. 4, the received voltage should be about 48 mv; this signal was measured with the Hewlett-Packard Model 302A Wave Analyzer and was actually 60 mv. Typically wideband series of 10 v peak measured from the loop-preamplifier combination indicated a field strength of 0.5 v/m. An average effective height of 20 m was indicated (Fig. 9).

The measurements made of these components indicate that they are sufficiently linear and accurate for use in superdirective arrays over the 10 to 30 kc frequency range.

MIXERS

LOOP ARRAYS MIXERS

The signals from the loops must be fed into a mixer, where they are delayed and subtracted with the least possible errors or differences in phase and amplitude. The No. 1 Emitter Follower Mixer (Fig. 10) built for the two-loop array has the following characteristics:

a. Depending on the amount of delay inserted, 12 to 20 v peak-to-peak is the maximum input voltage before distortion occurs.

b. Also depending on the delay, the loss (Fig. 11) through the mixer is from 7 to 11.5 db.

c. The delay variation over a wide range of frequencies before and after compensation is shown in Figs. 12 and 13, respectively.

d. The net voltage change between east and west channels (Fig. 13) limits the null depth over a wide frequency range.

e. The nulling capabilities can be computed from the data in Fig. 13. When the array was nulled at 20 kc with 5.2 μ sec delay inserted, the mixer nulled -26 db at 10 kc and -20 db at 30 kc. When using a sine wave nulled -51.3 db at 20 kc with 2.4 μ sec delay inserted, the mixer nulled -23 db at 10 kc and -25 db at 30 kc. A typical sferic generated by the function generator was nulled -34 db. It is concluded that the delay error determines the null depth at the higher frequencies, and the amplitude error determines the depth at the lower frequencies.

The mixer was installed at the Johnson Valley field site. Two loops placed 1 mi apart were used for a superdirective array; the array was nulled on Navy VLF station NAA (18.6 kc, 60 deg true bearing) and two patterns (Figs. 14 and 15) were taken with the passive pattern plotter (PPP) at 10.5 kc (Ref. 5). The large back lobes shown in the figures are results of nulling 50 deg off the axis of the array. The figures also show that pattern repetition was very good.

SHORT BEVERAGE ARRAY MIXER

An improved mixer that uses higher impedance delay lines was designed and tested for use in a superdirective Beverage array (Fig. 16). The characteristics of this No. 2 Emitter Follower Mixer are:

- a. The maximum input voltage before distortion is 15 v peak-to-peak.
- b. The loss through the mixer is 8 db. The net voltage output between east and west channels over a wide frequency range is shown in Fig. 17.
- c. The net phase delay, in microseconds, between east and west channels is given in Fig. 18.
- d. The nulling capabilities can be computed from the foregoing data by using the equation $E_n = \Delta e^{-j\Delta\theta/L_1}$. With the mixer nulled at 20 kc, the null voltages at 10 kc and 30 kc should be -37.4 db and -25.7 db, respectively. Fair agreement was obtained when a simulated superdirective array was connected to the mixer, which was nulled at 20 kc. The null was -35.5 db at 10 kc and -29.5 db at 30 kc. The typical sferic generated by the function generator was nulled -34 db.
- e. The mixer was installed at the Johnson Valley site; two Beverage antennas one-half mile in length and at 115 deg relative orientation were installed to form a superdirective array. The array was nulled on three Navy VLF stations, with the following results:

Station NAA (18.6 kc, 60 deg true bearing), null -40 db

Station NSS (22.4 kc, 70 deg true bearing), null -34 db

Station NPM (19.8 kc, 265 deg true bearing), null -32 db

With the array nulled on NAA and using sferics, a 10.5 kc pattern (Fig. 19) was made with the PPP. The large back lobe shown is a result of nulling 60 deg off the axis of the array. An improved pattern (Fig. 20) was taken under similar conditions, but with the antennas terminated in their characteristic impedance and the array nulled beforehand on sferics arriving from 70 deg true. Under these conditions, nulls 25 db below the main lobe were recorded, and the back lobes were down 17 db. Another pattern (Fig. 21) was taken under like conditions, but with the array nulled at 110 deg true; nulls 28 db below the main lobe, and back lobes 19 db below the front lobe, were recorded. The 18 db side lobes are approximately what would be expected from the theoretical pattern of such an array. Three elements (-30 db back lobes) must be used to obtain lower back lobes. Another pattern (Fig. 22) was taken under the same conditions, but from the east-looking output of the mixer. Therefore, the pattern shows nulling on the axis of the array to the west at 290 deg true.

- f. The input impedance of the No. 2 Mixer was $365-j82$ for the east input, and $370-j85$ for the west; the inputs are not purely resistive at 20 kc.

g. For the mixers, a calibration of net delay as a function of inserted delay is given in Fig. 23. The net delay is very close to the inserted delay selected by the delay lines.

h. The Beverage antennas were terminated with their characteristic impedances (Z_0). To determine the impedance, the load resistance on the antenna was increased until maximum power was delivered; a resistance value of approximately 270 ohms was indicated (Fig. 24). Resistance was then placed at the far terminations of the Beverage antennas to balance the termination and ground-plane resistances, thus providing the proper antenna termination impedance. The west antenna required 250 ohms, and the east 200 ohms. Input impedance measurements were made to confirm the frequency-response flatness of the Beverage; the results are plotted in Fig. 25, where Z_0 is a nominal 280 ohms.

TRANSMISSION LINE CHARACTERISTICS

If the connecting transmission lines are not terminated in their characteristic impedances, pattern deterioration can result. Fig. 26 shows that the phase delay can change markedly with variances in termination resistance on a typical coaxial cable, RG58/U. Fig. 27 is a plot of the losses and phase delays through RG58/U and RG22/U cables, over a wide frequency range. The figure shows that, if the cables are not terminated in their characteristic impedances of 53 ohms and 48 ohms, respectively, with the center conductors connected, the losses and phase delays vary with frequency. Usually, a termination resistance above Z_0 causes the phase delay to increase, and the loss to decrease, with frequency. If the termination resistance is below Z_0 , opposite effects are observed.

CONCLUSIONS

Any error in phase or amplitude tends to deteriorate the pattern of a superdirective array. Therefore, if the array is designed to operate over a broad band of frequencies such as 10 to 30 kc, each array component must be scrutinized.

In a broadband mixer, the phase errors deteriorate the null depths at the higher frequencies; at the lower frequencies, the null depths are deteriorated by the amplitude errors.

High directivity was achieved with superdirective loop and Beverage arrays that employed the components described in this report.

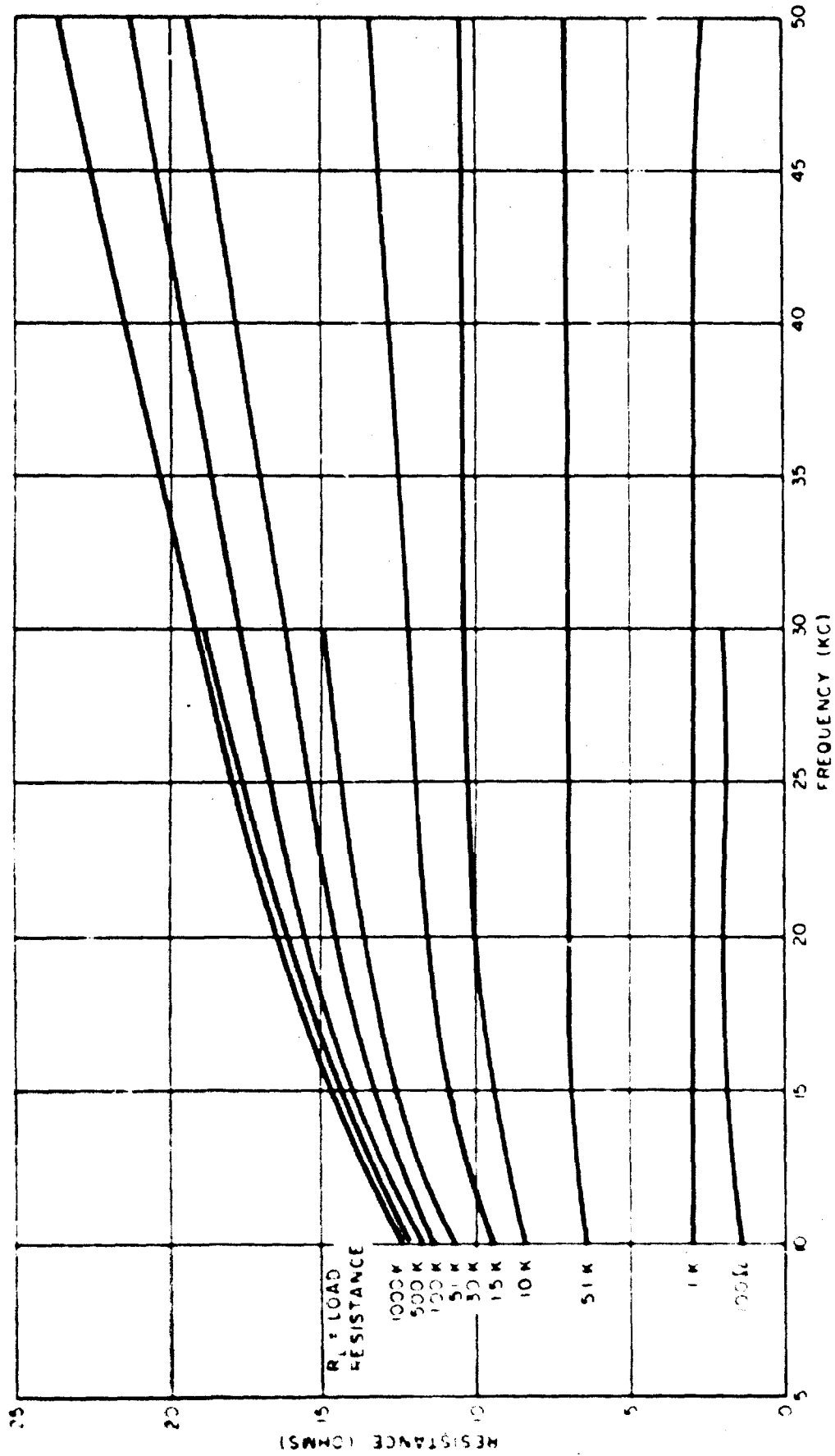


FIGURE 1. Input Impedance of Z-100-134 Transformer

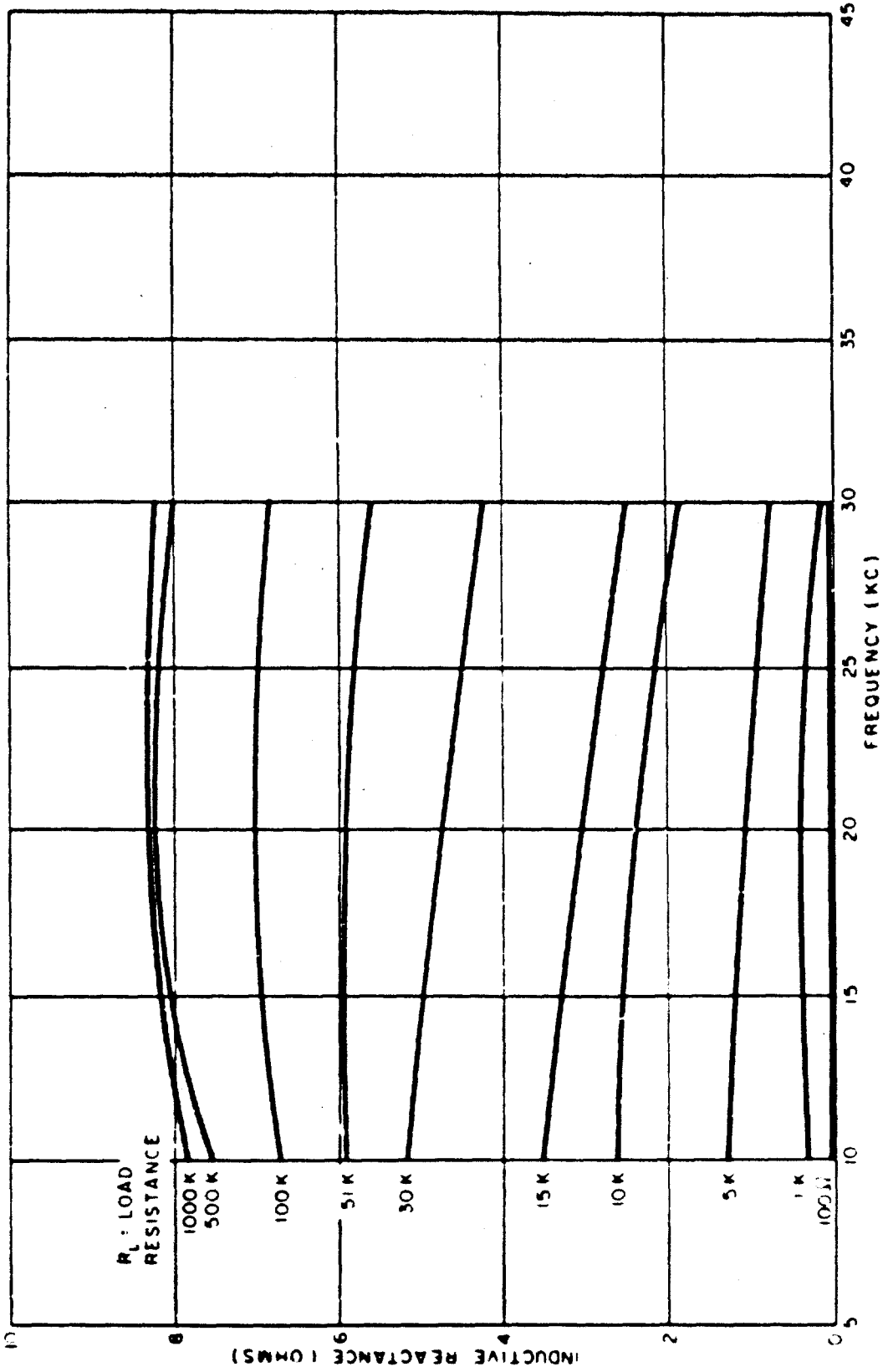


FIGURE 2. Input Reactance of Z-100-134 Transformer

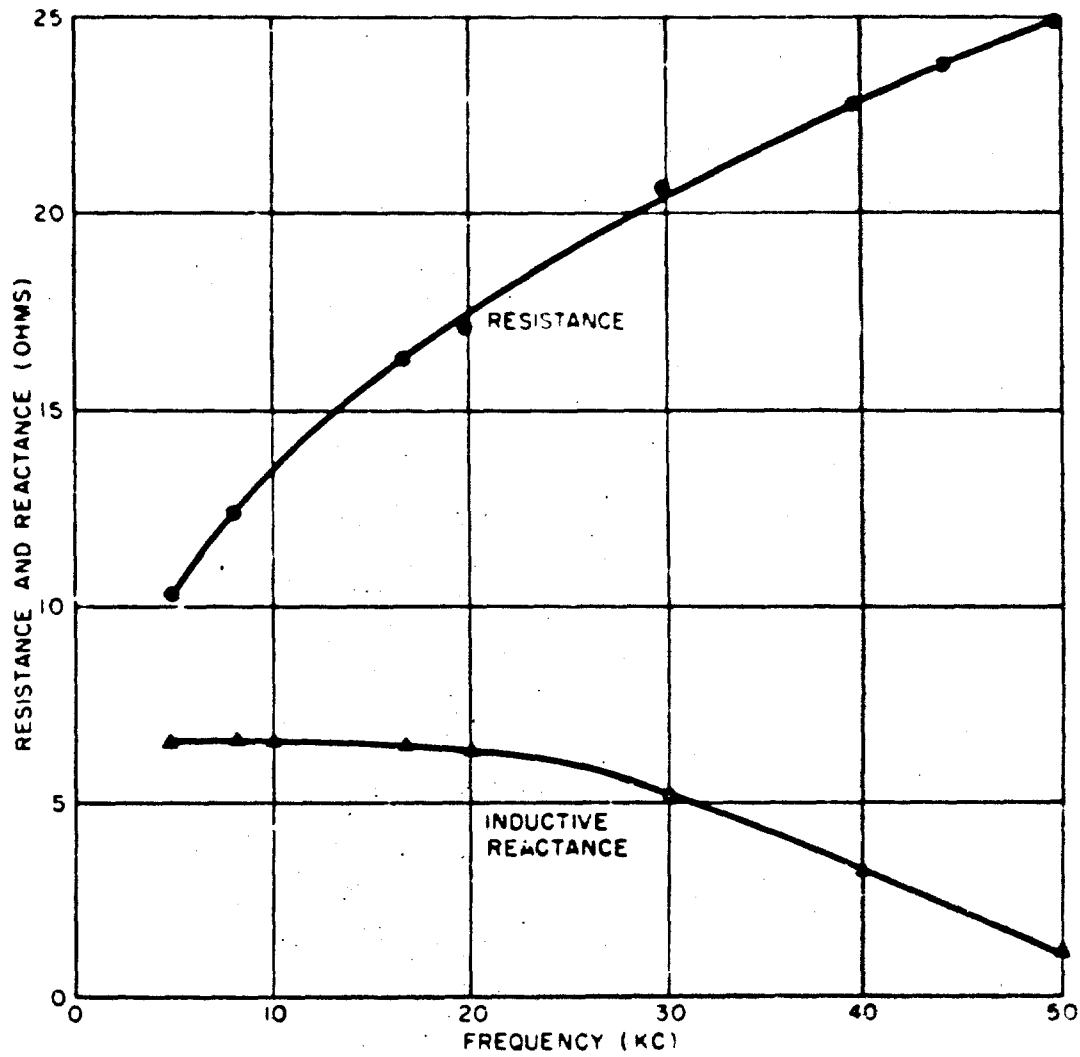


FIGURE 3. Loop Preamplifier Input Impedance;
 Amplifier With NE-134 Matching Transformer

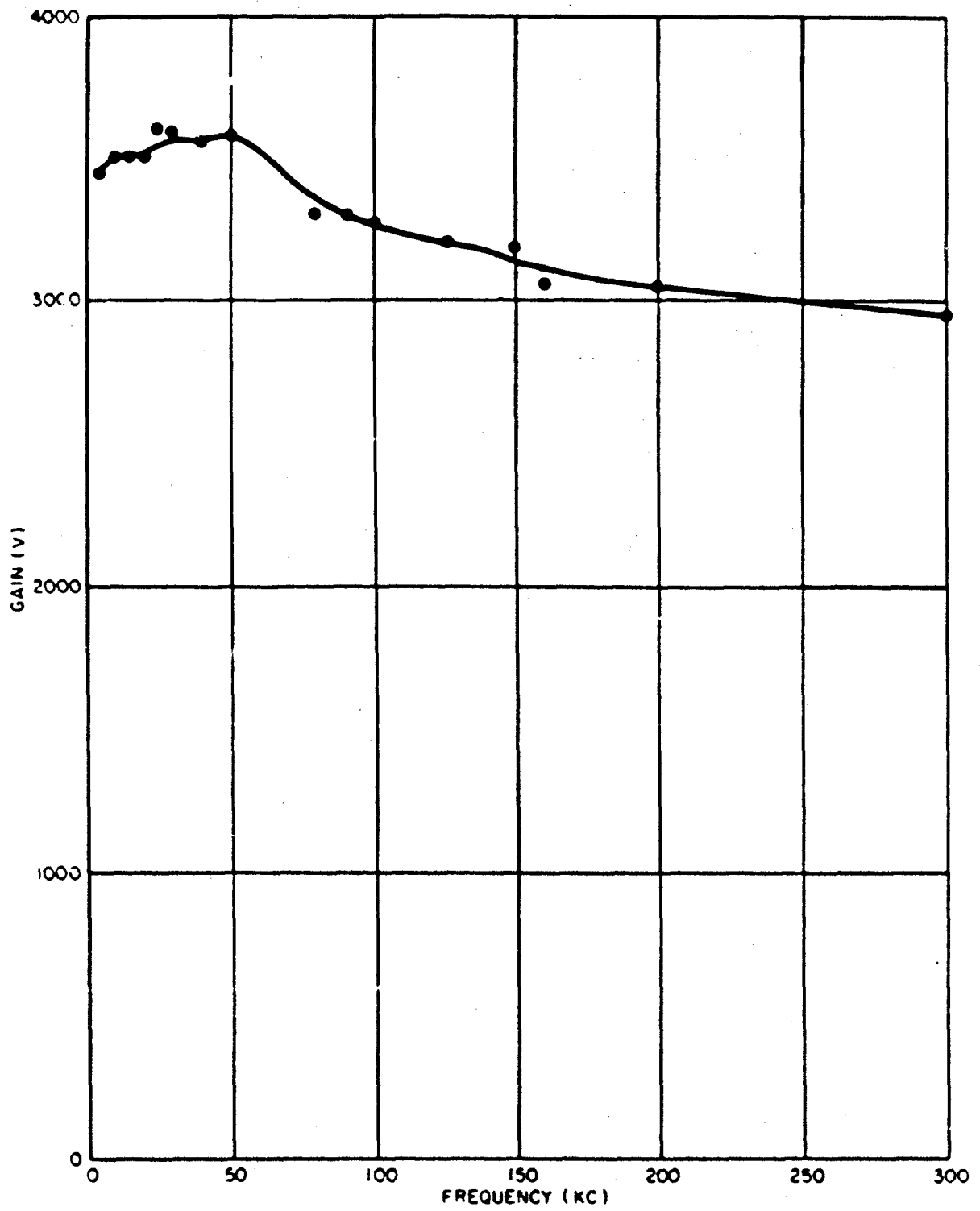


FIGURE 4. Preamplifier and Transformer Gain

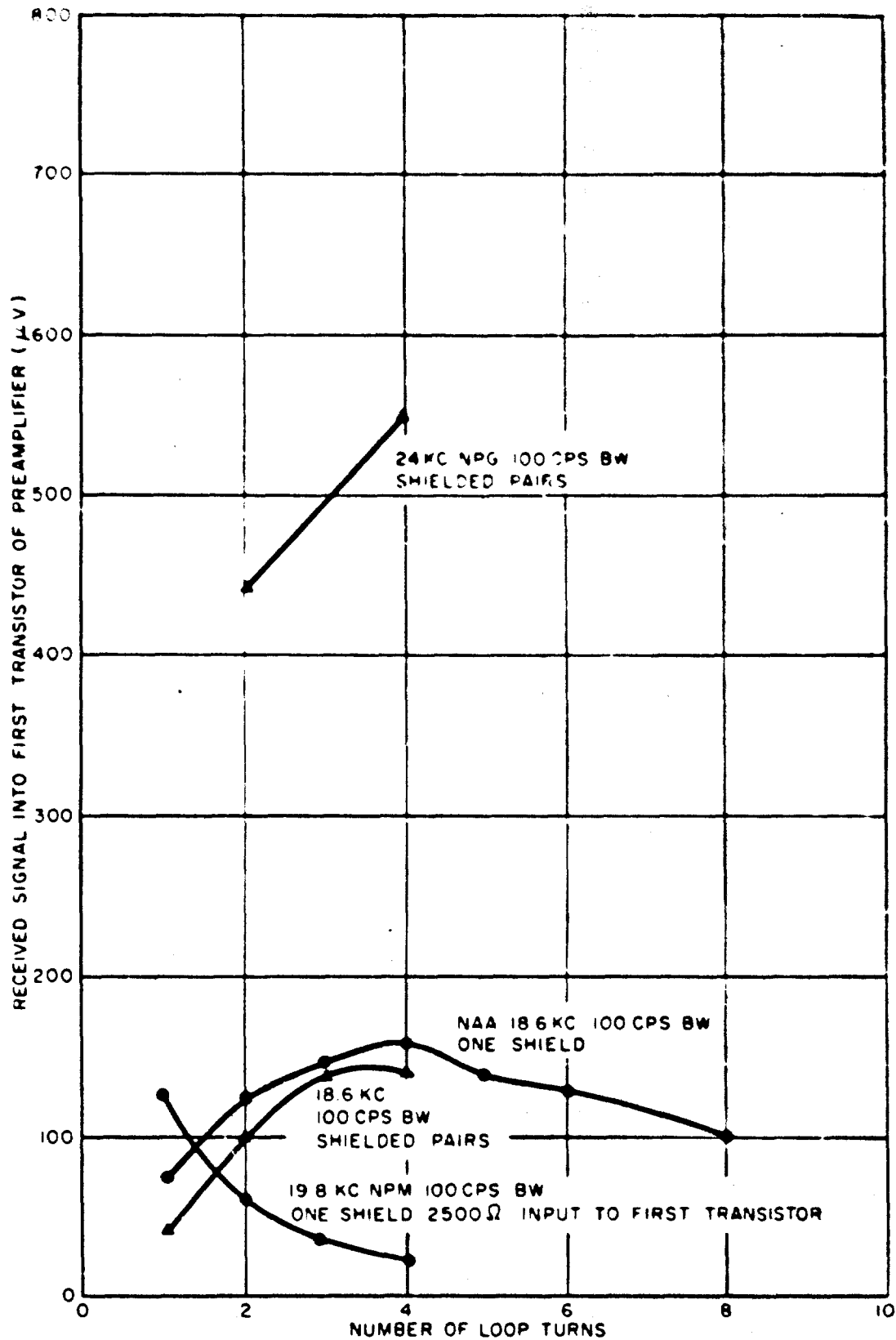


FIGURE 5. Comparative Reception of Loops 10 ft Square

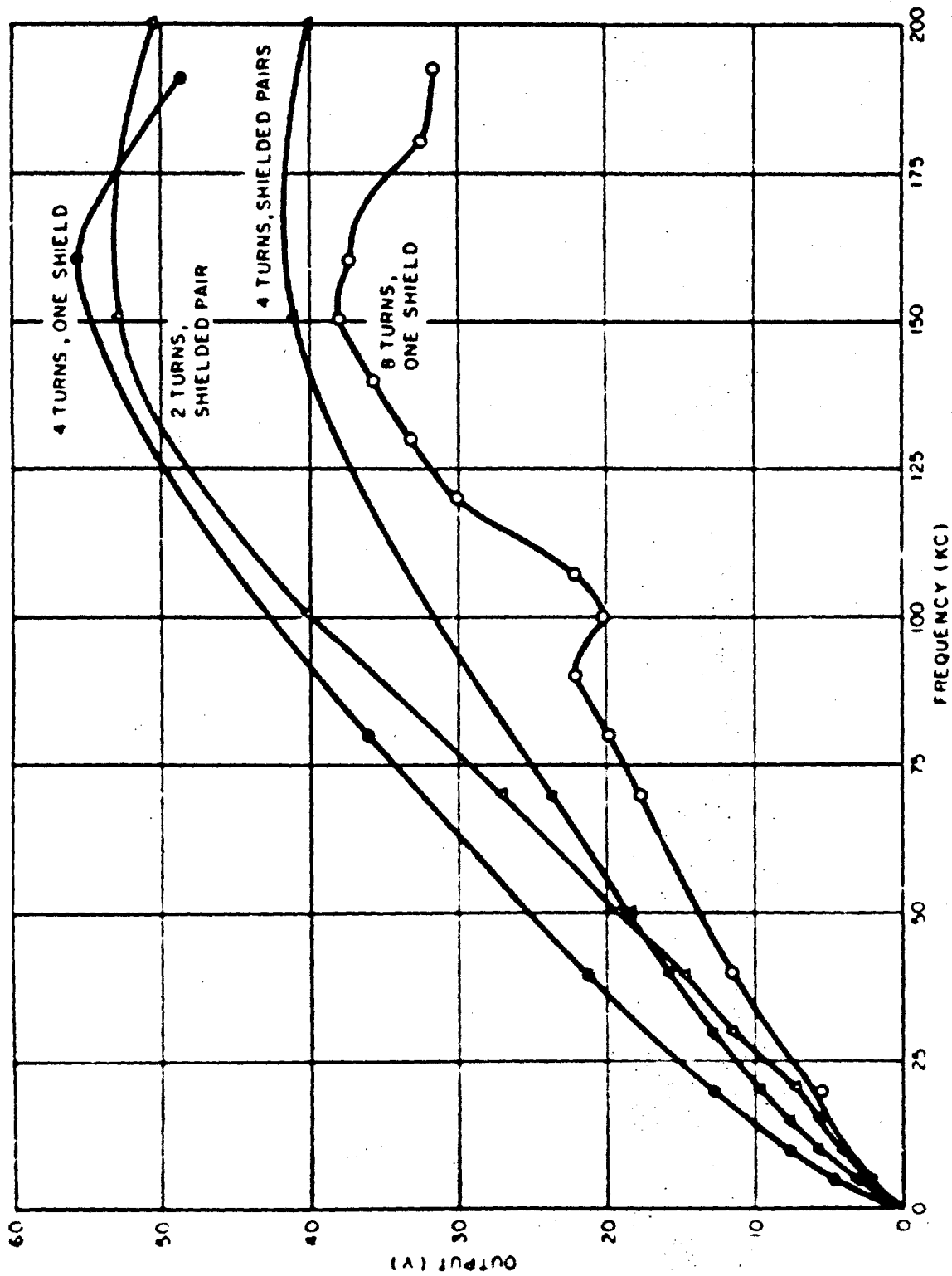


FIGURE 6. Loop 10 ft Square With Constant 15 ma Input to Transmitting Loop

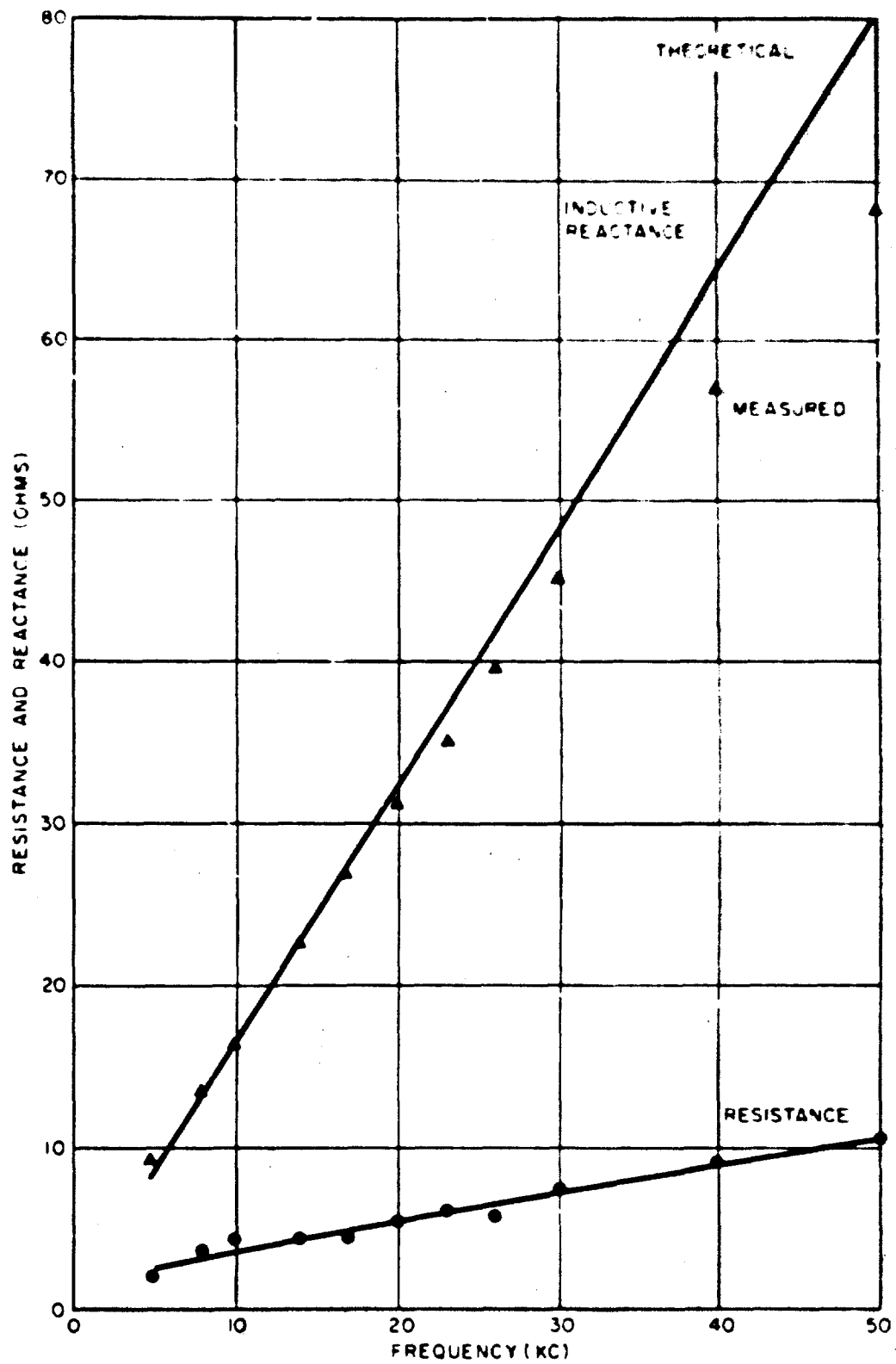


FIGURE 7. Input Impedance of Loop 10 ft Square With Four Turns

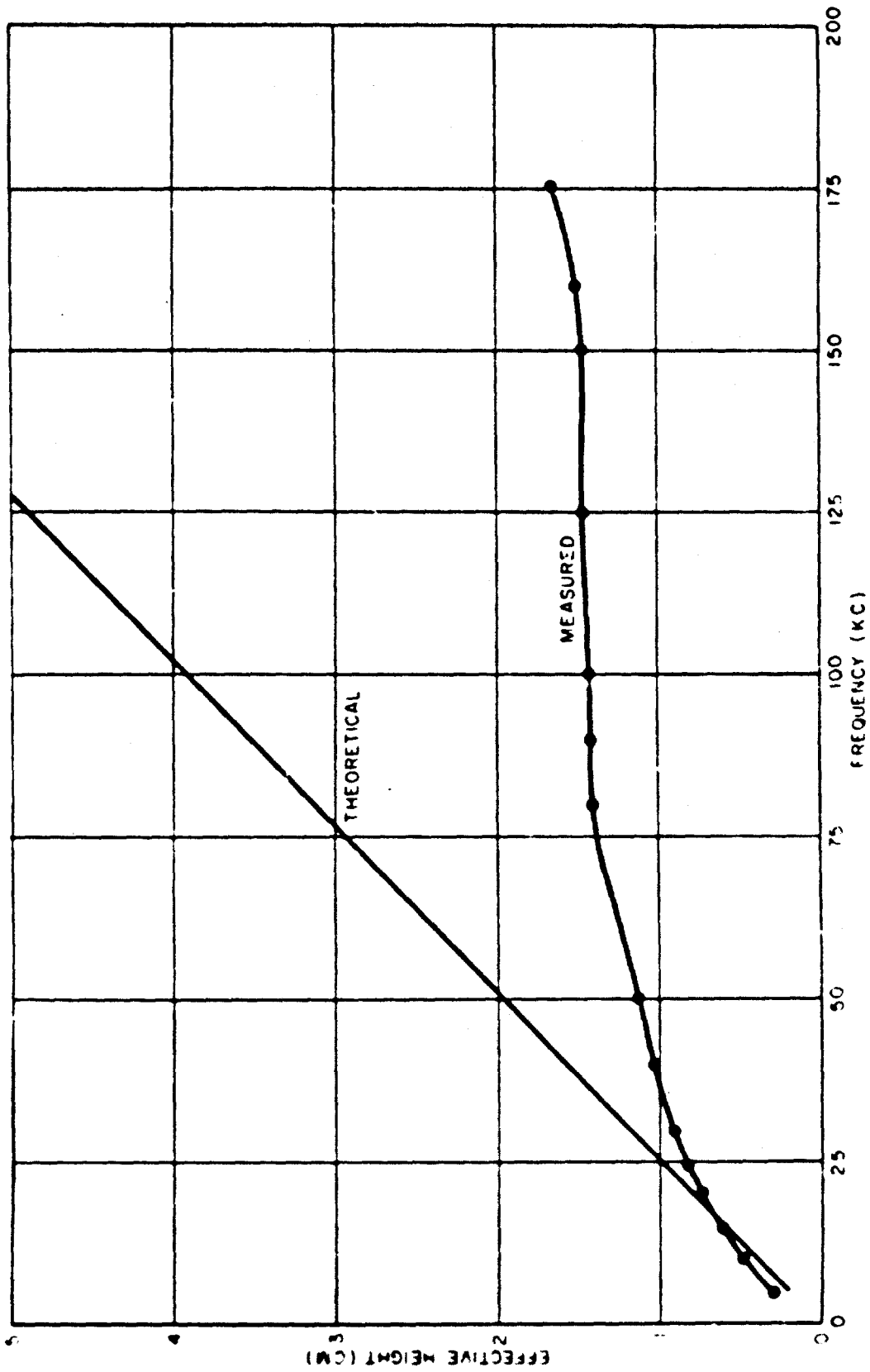


FIGURE 8. Effective Height of Loop 10 ft Square With Four Turns

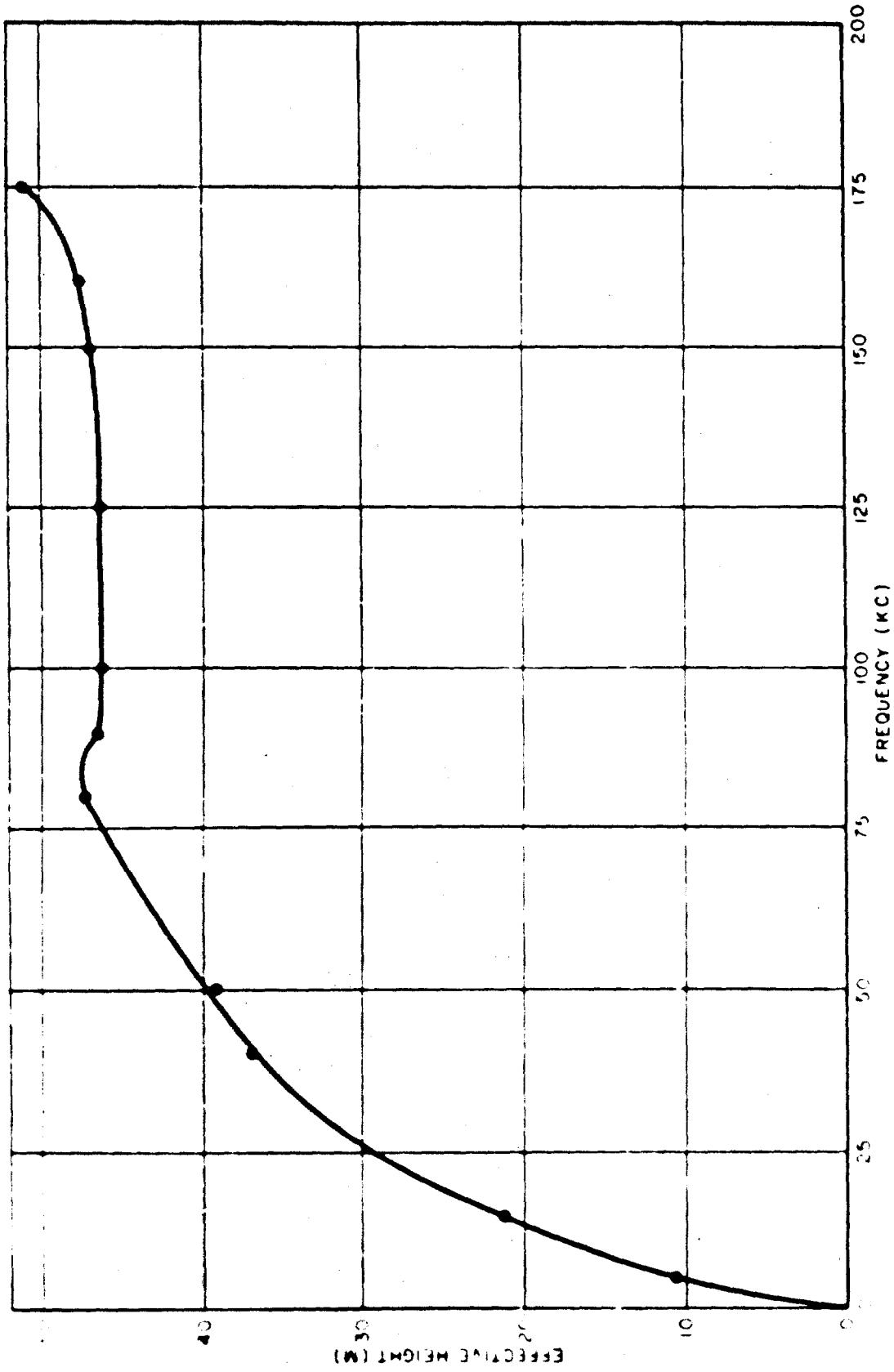


FIGURE 9. Effective Height of Loop 10 ft Square With Four Turns and Preamplifier Terminated in 100 Ohms

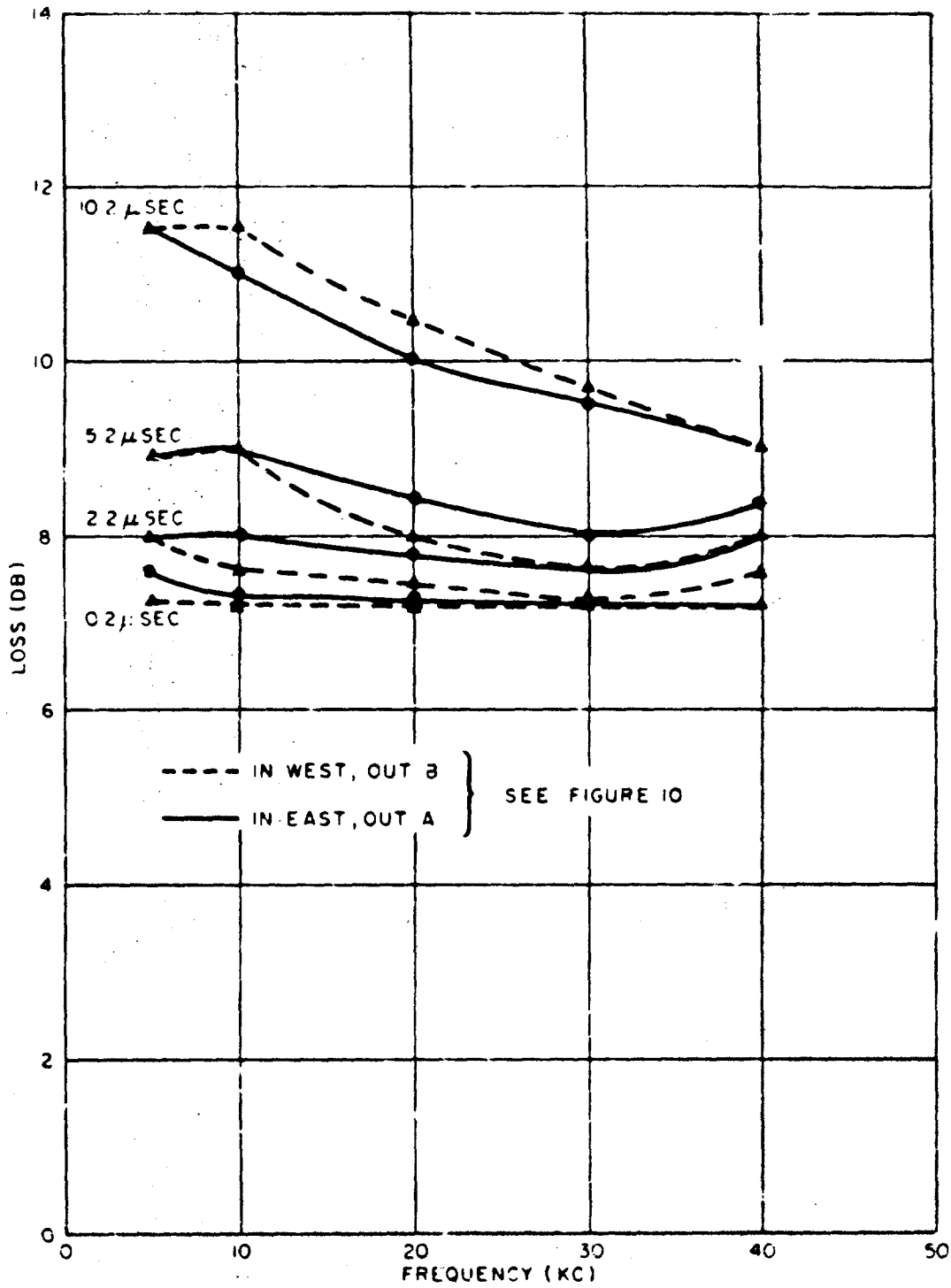


FIGURE 11. Loss Through No. 1 Emitter Follower Mixer

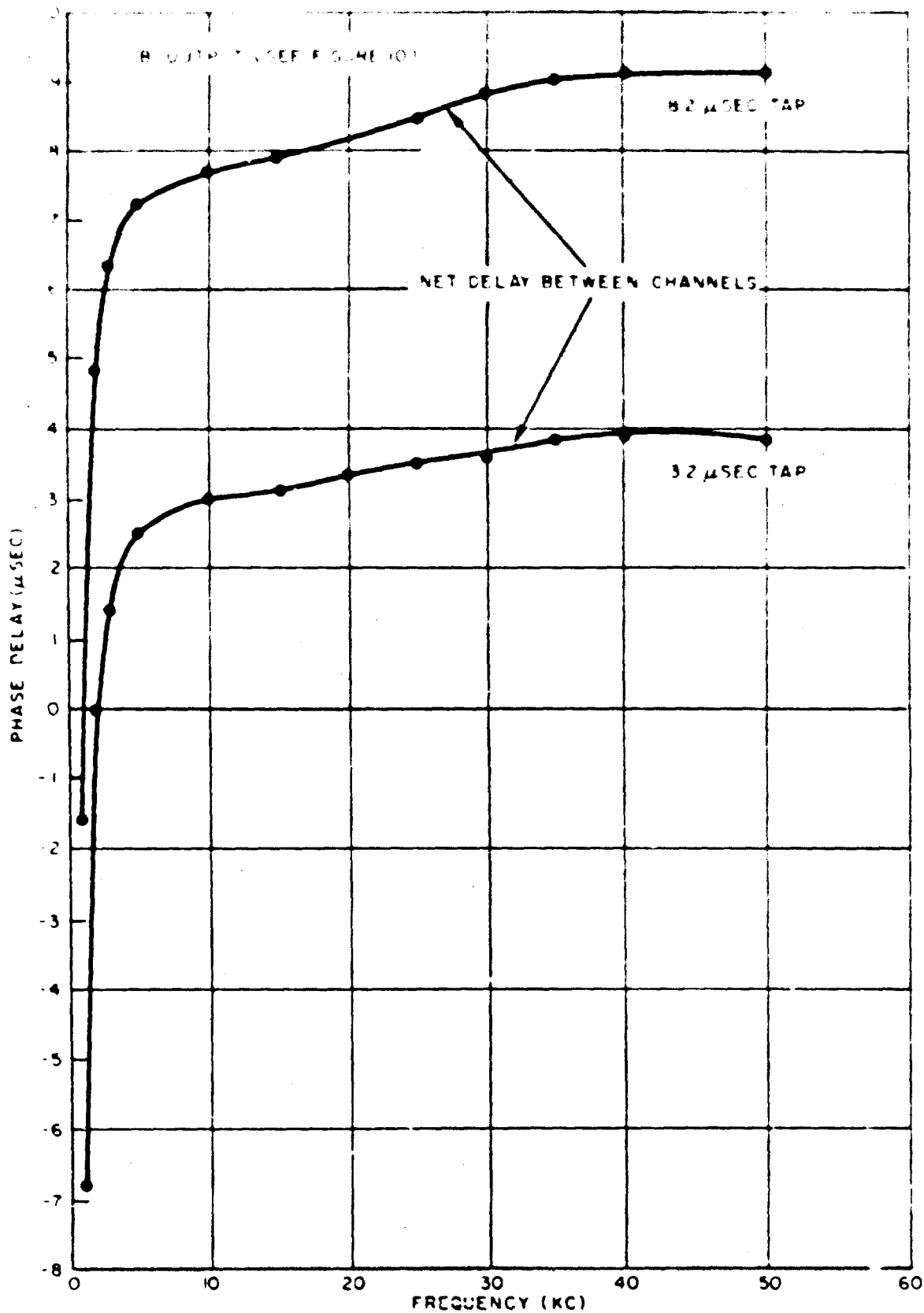


FIGURE 12. Phase Delay Before Compensation Through No. 1 Emitter Follower Mixer

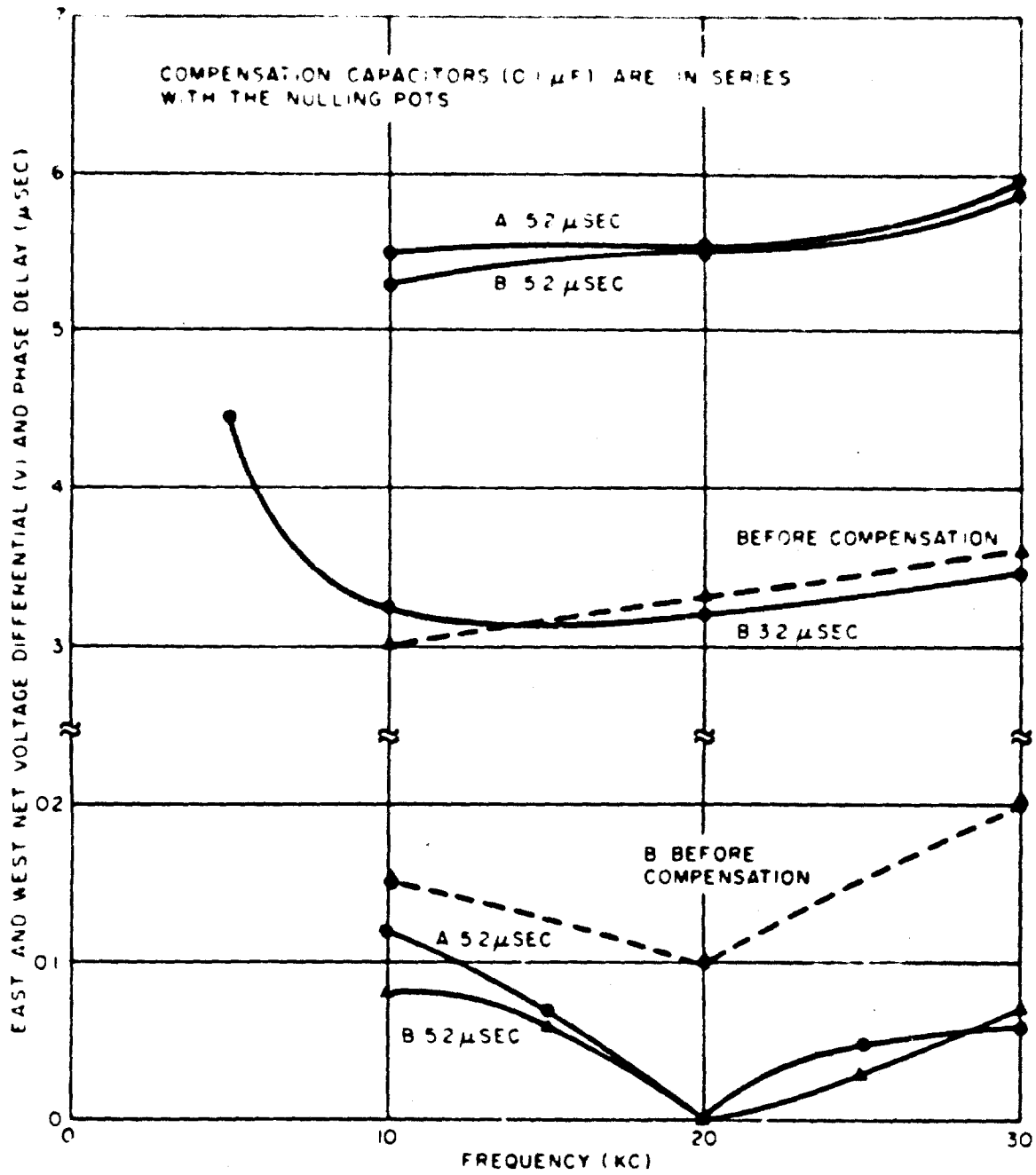


FIGURE 13. Phase Delay Through and Voltage Differential in No. 1 Mixer

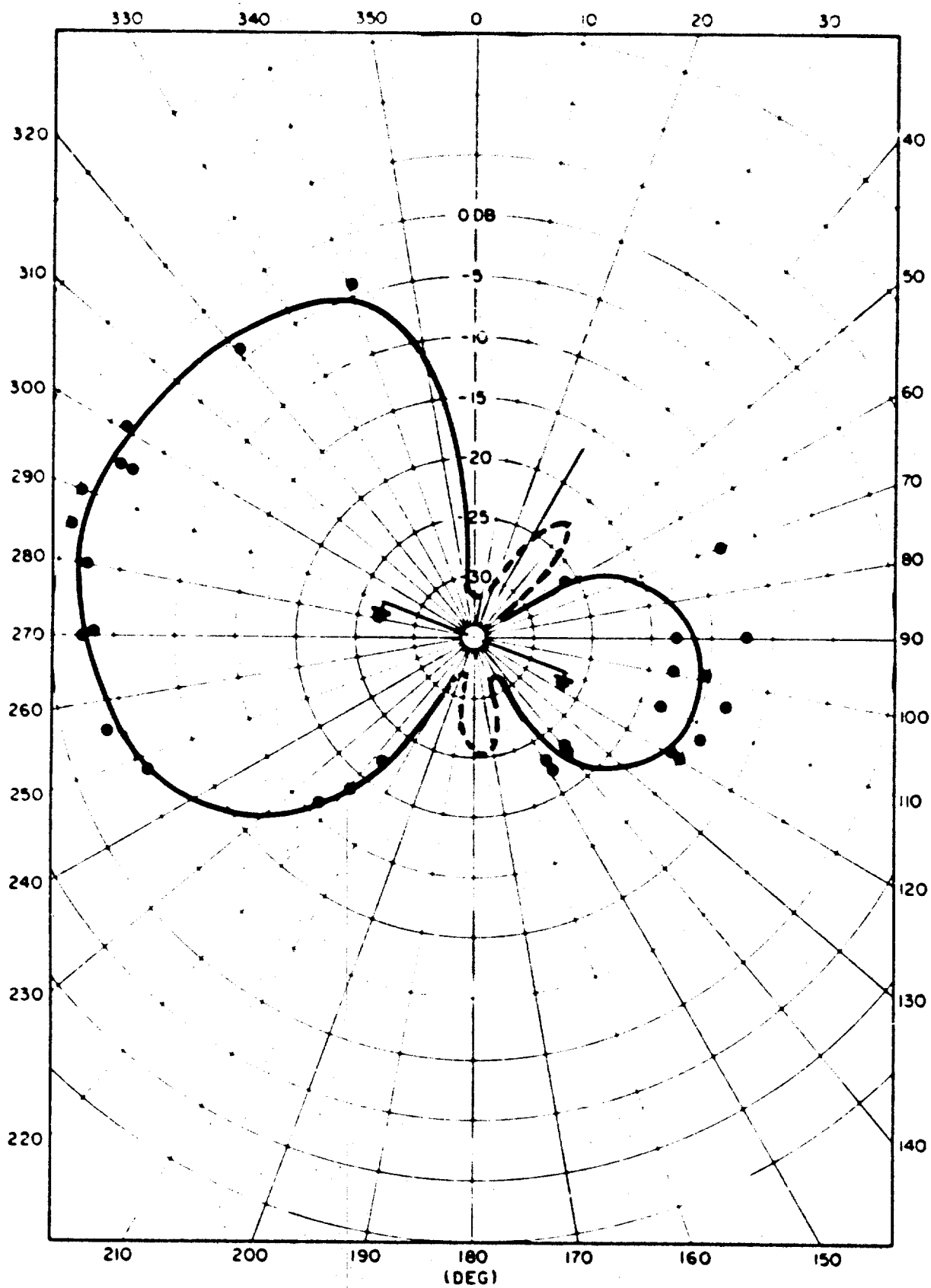


FIGURE 14. Reception Pattern of Two-Loop Array

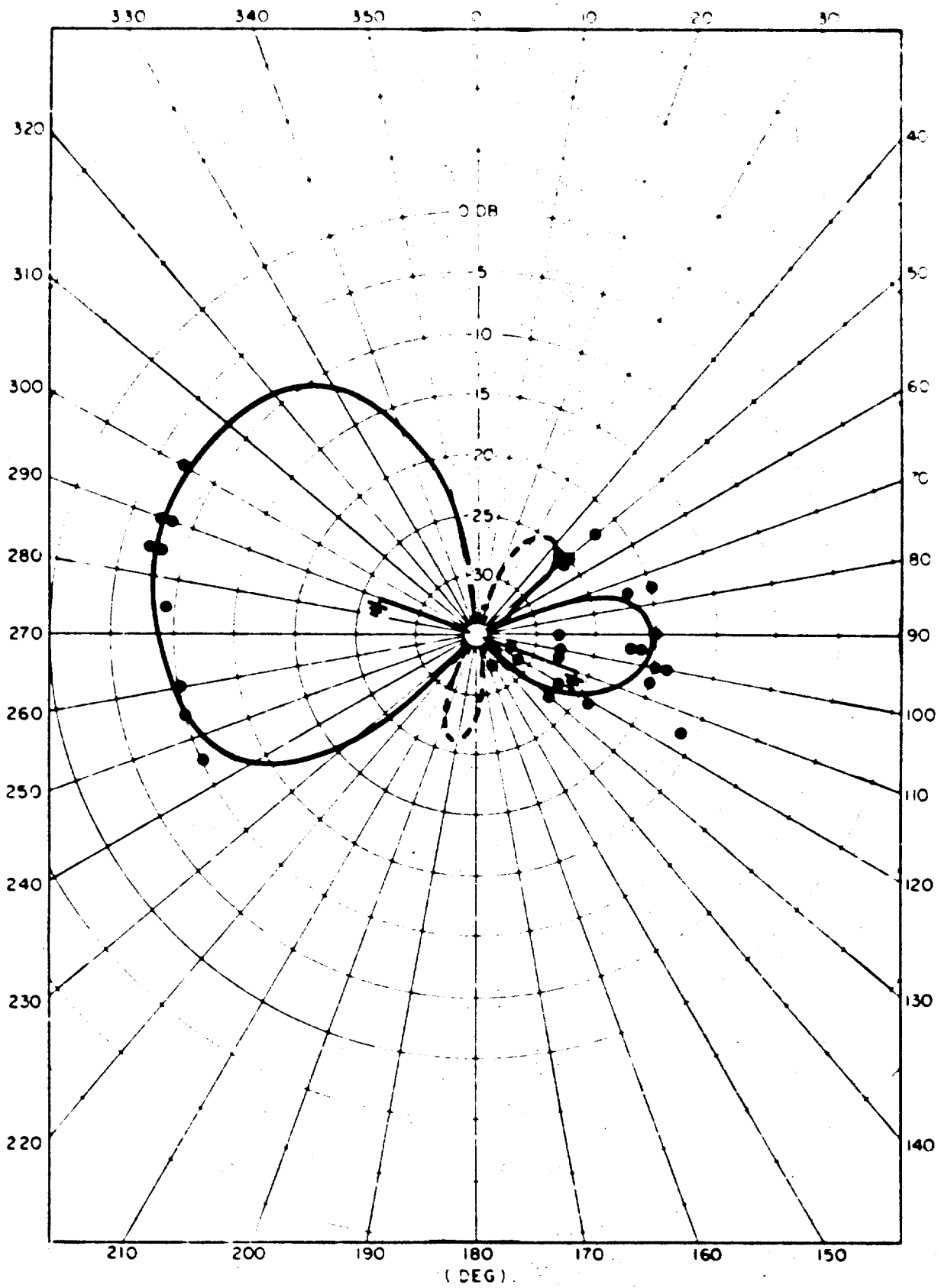


FIGURE 15. Reception Pattern of Two-Loop Array

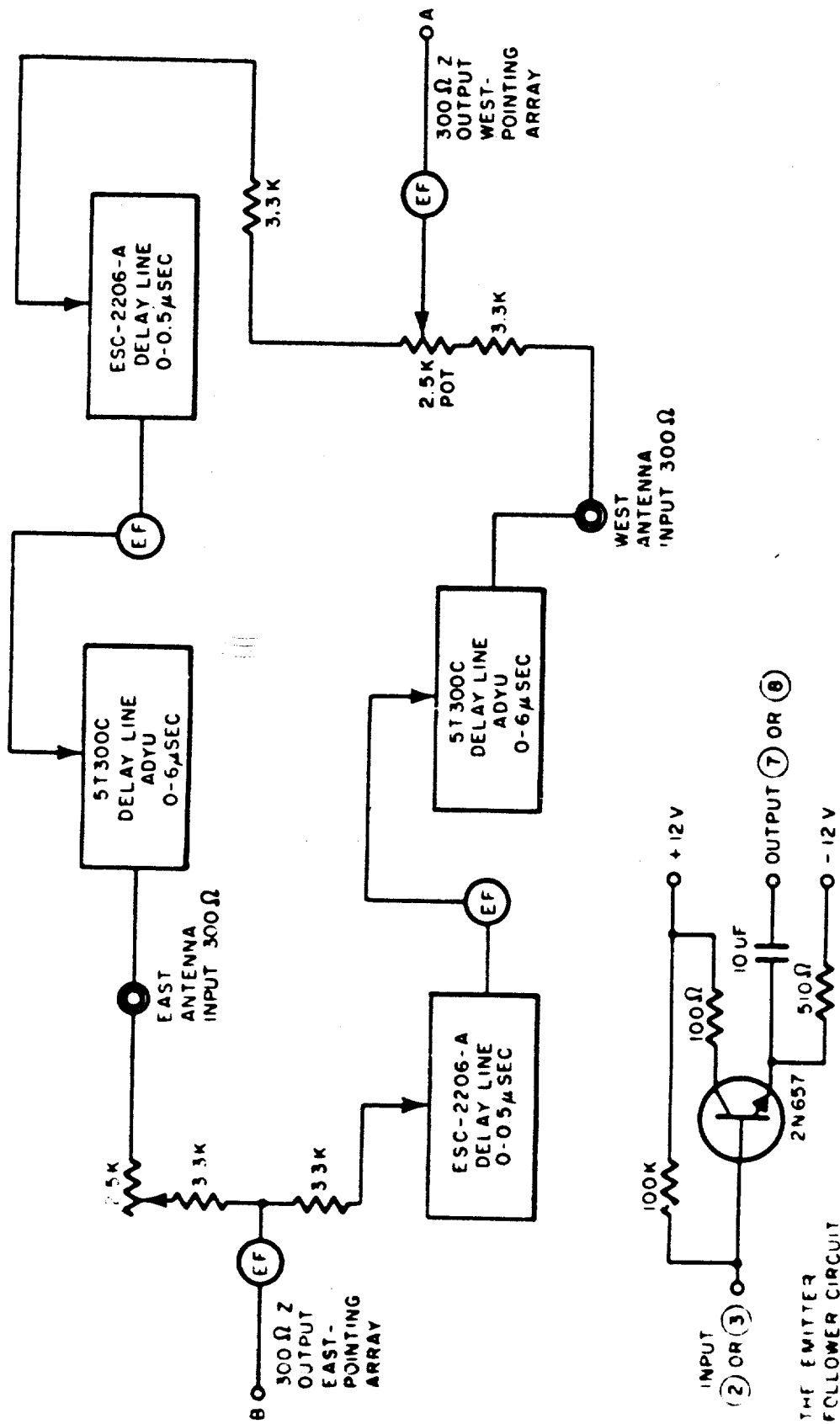


FIGURE 16. No. 2 Emitter Follower Mixer for Superdirective Array

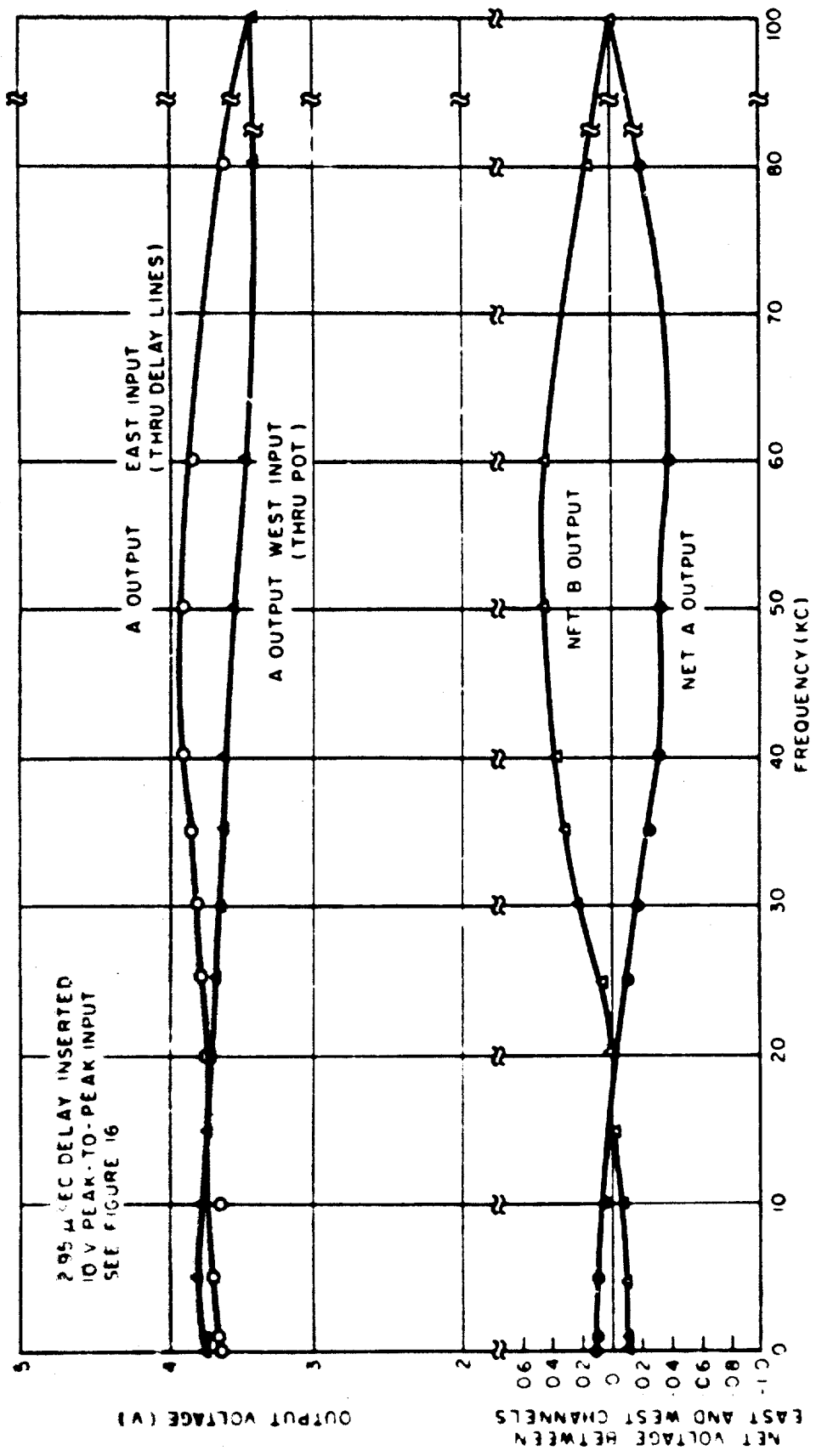


FIGURE 17. Loss Through No. 2 Emitter Follower Mixer

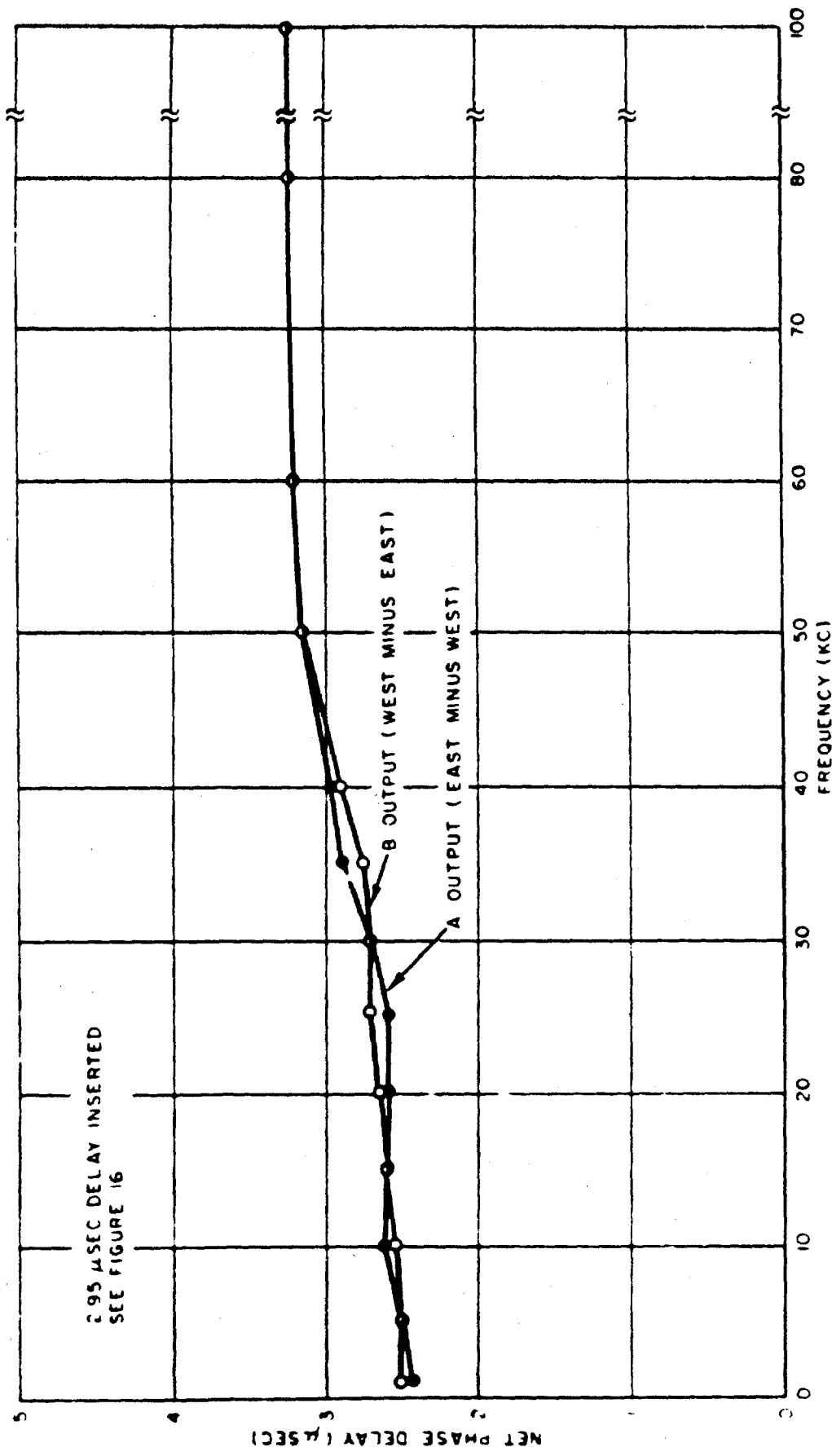


FIGURE 18. Phase Delay Through No. 2 Emitter Follower Mixer

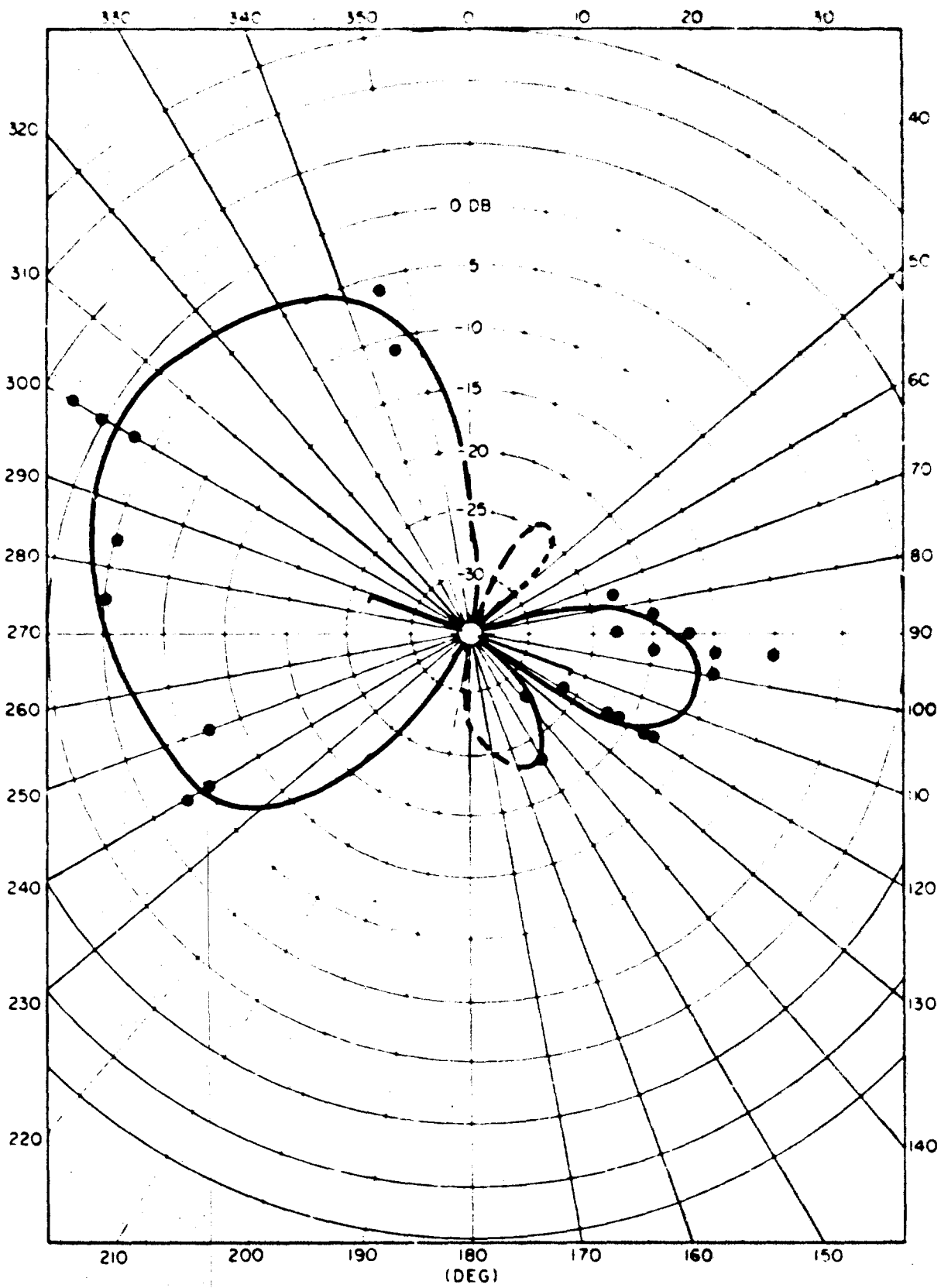


FIGURE 19. Reception Pattern of Two-Beverage Superdirective Array Nulled on 60 Deg and Open at Far Ends

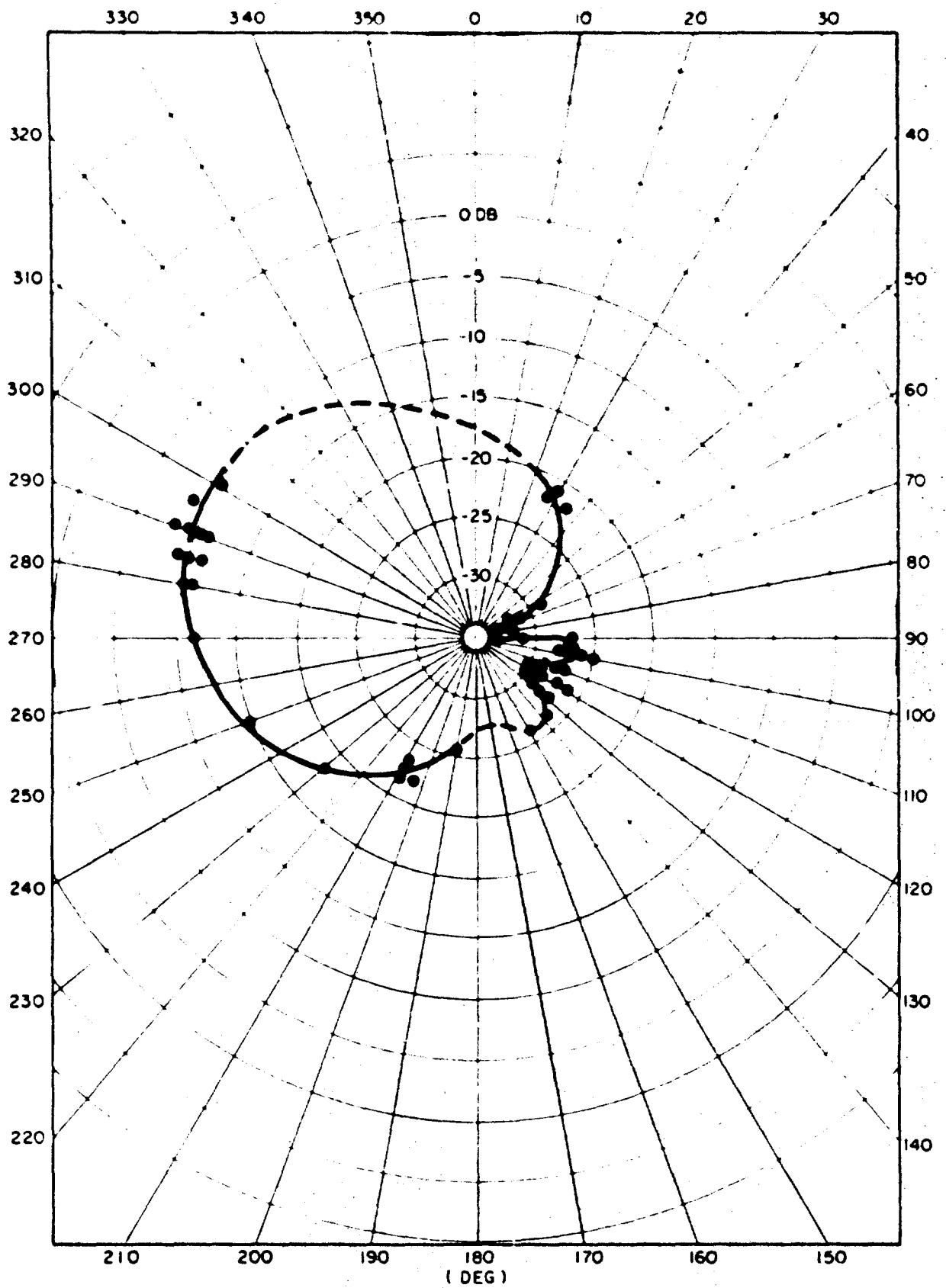


FIGURE 20. Reception Pattern of Two-Beverage Superdirective Array Nulled on 70 Deg and Terminated in Z_0

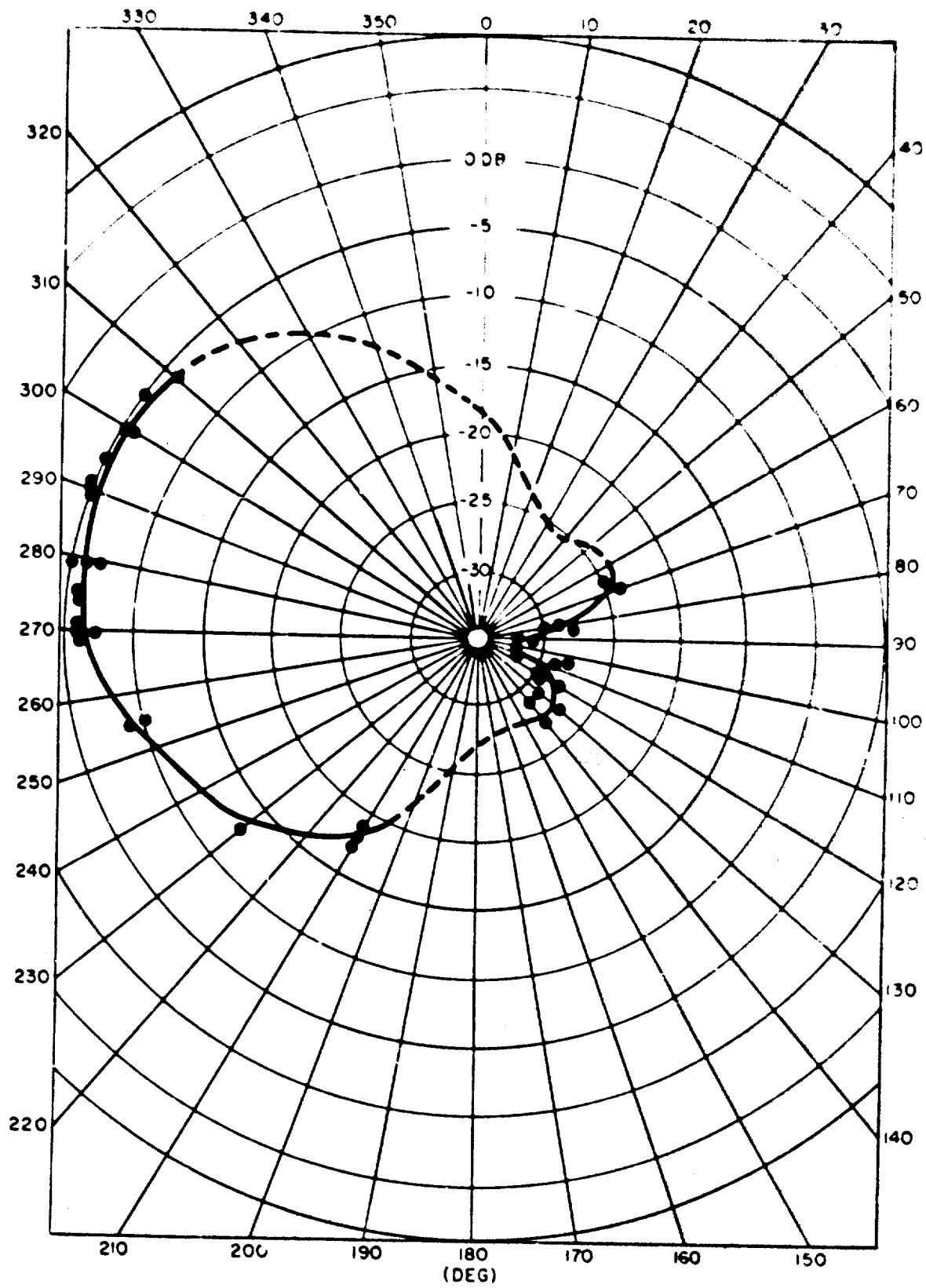


FIGURE 21. Reception Pattern of Two-Beverage Superdirective Array Nulled on 110 Deg and Terminated in Z_0

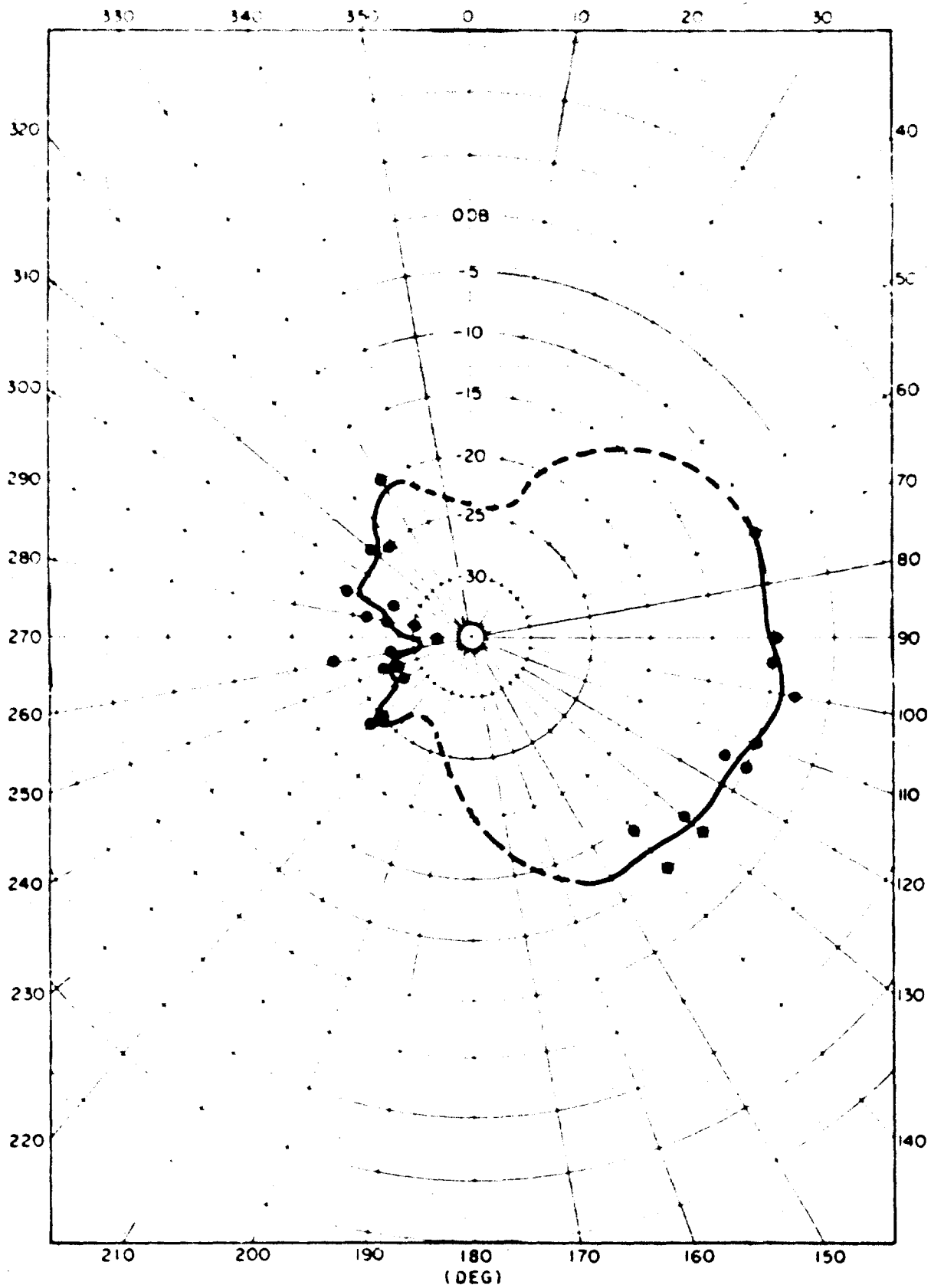


FIGURE 22. Reception Pattern of Two-Beverage Superdirective Array Nulled on 290 Deg and Terminated in Z_0

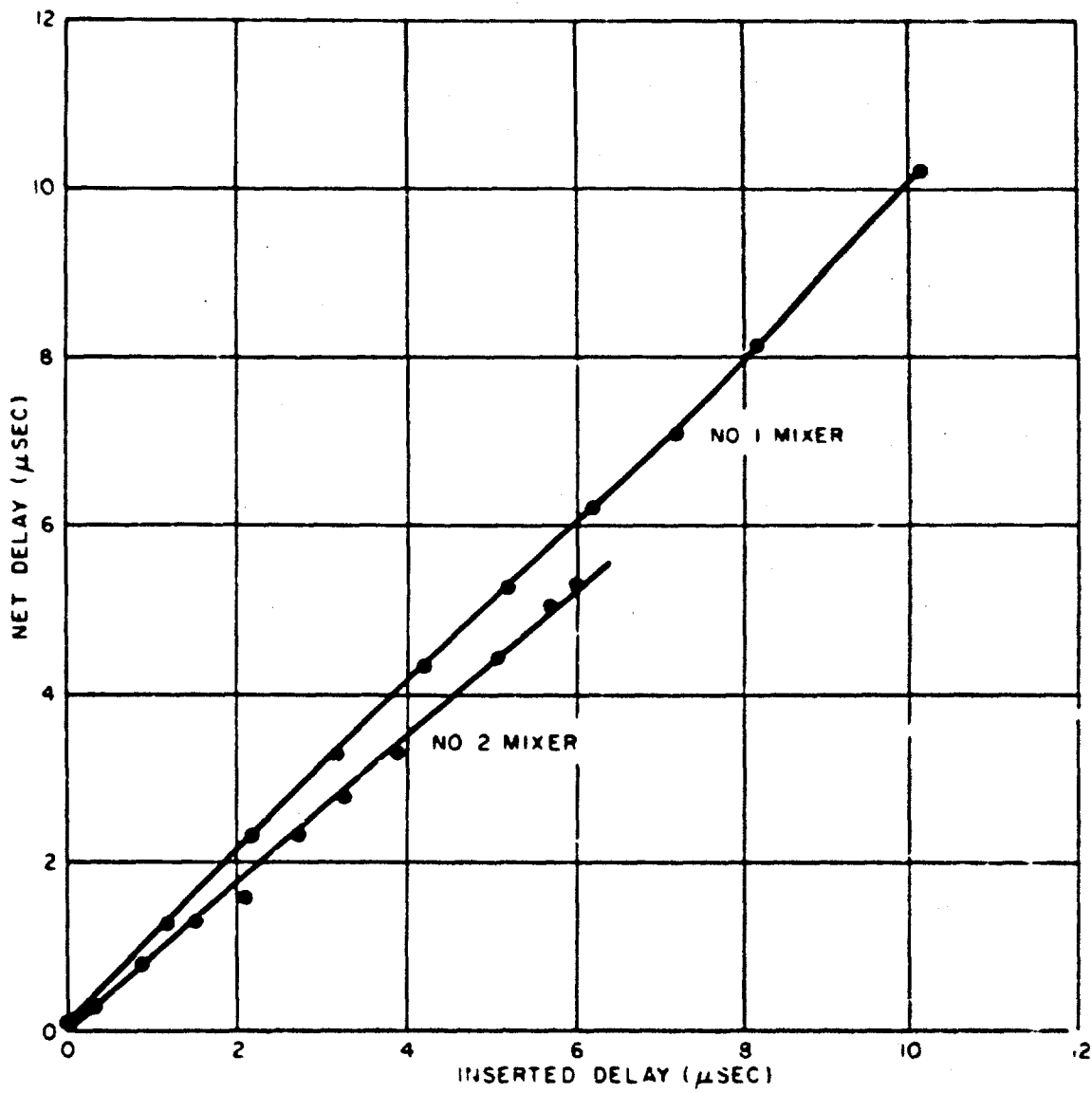


FIGURE 23. Phase Delay Calibration of Emitter Follower Mixers

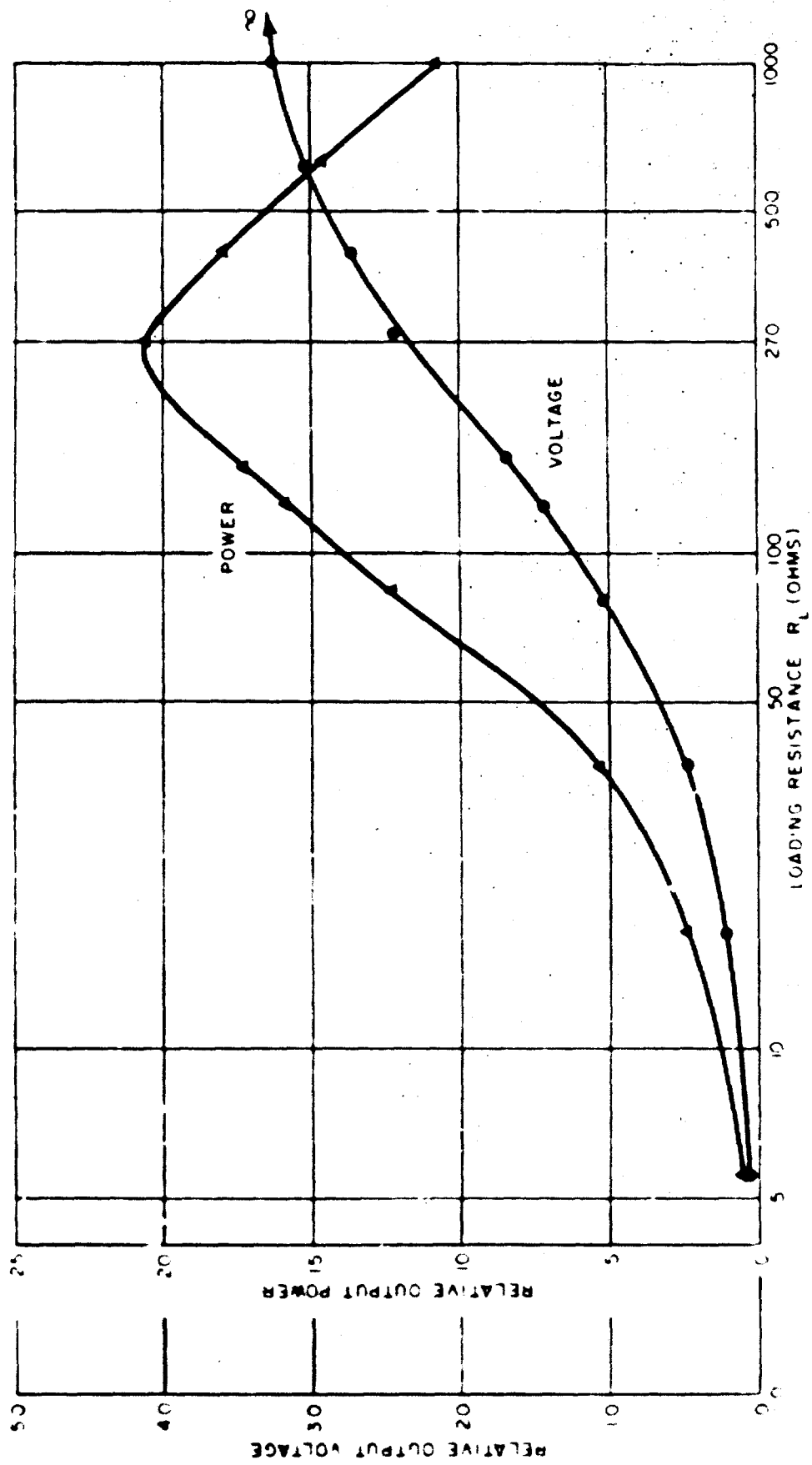


FIGURE 24. Voltage and Power Reception of Beverage Antenna

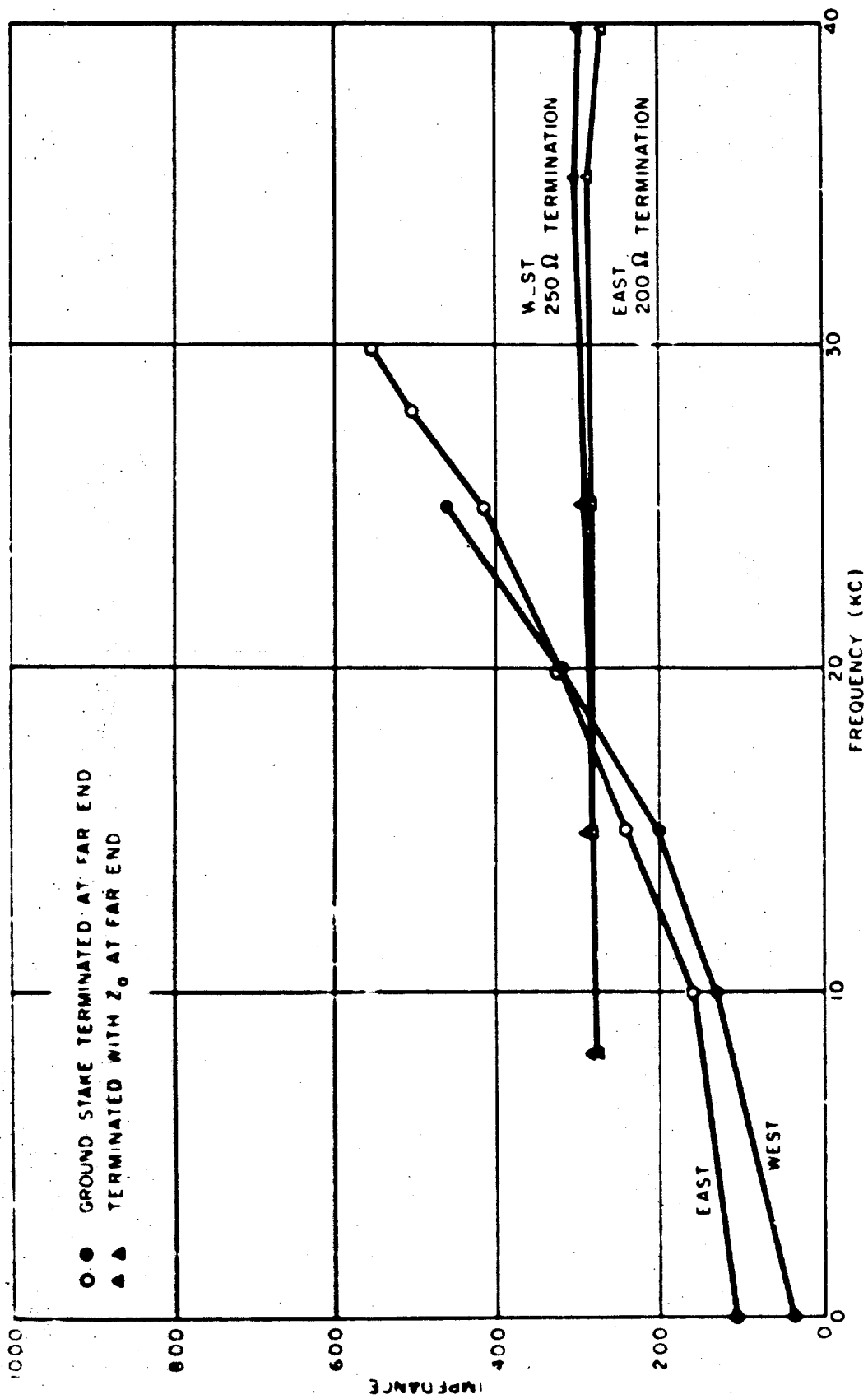


FIGURE 25. Frequency Response of Beverage Antennas One-Half Mile Long

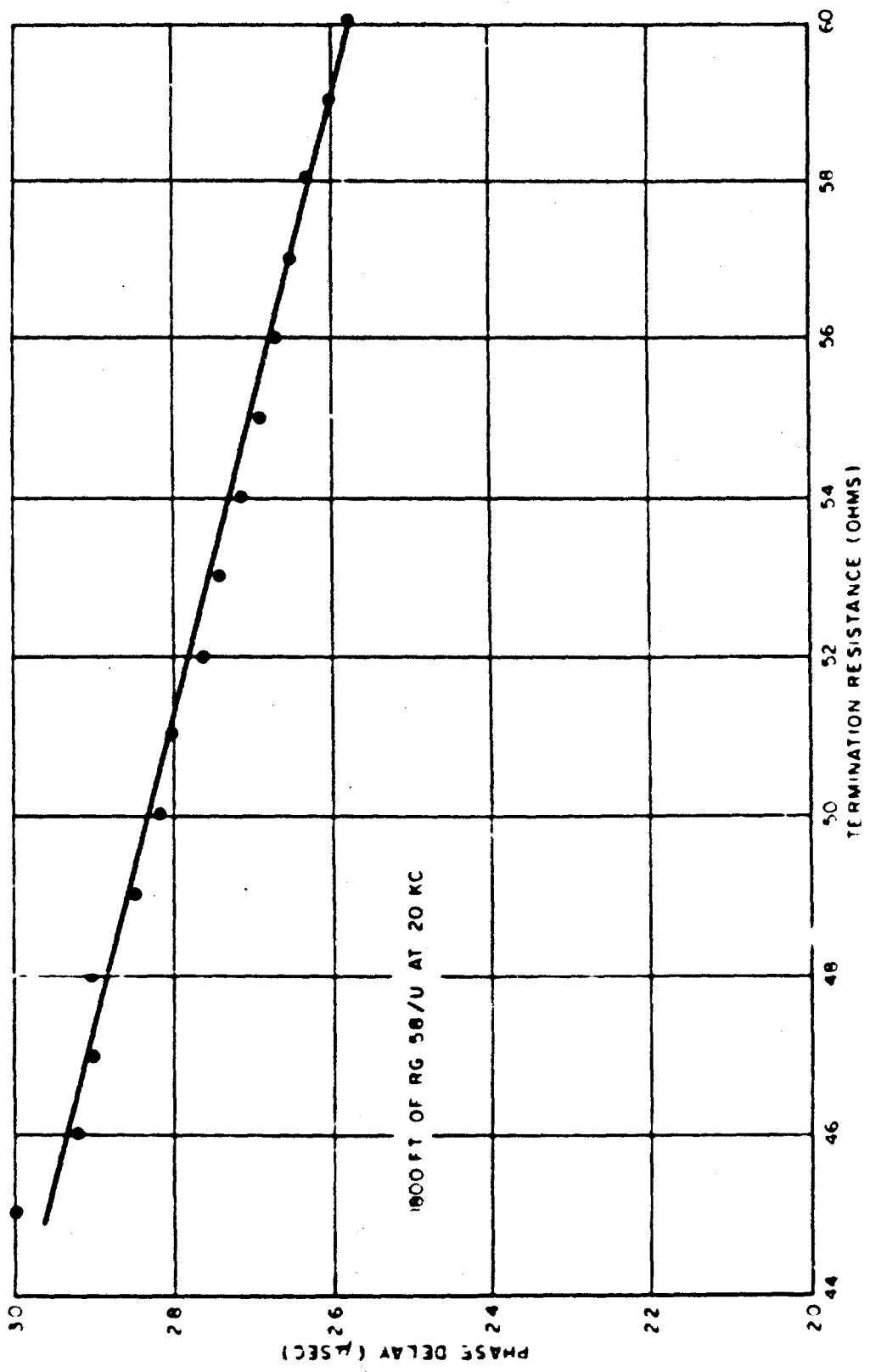


FIGURE 26. Phase Delay Through Coaxial Cable

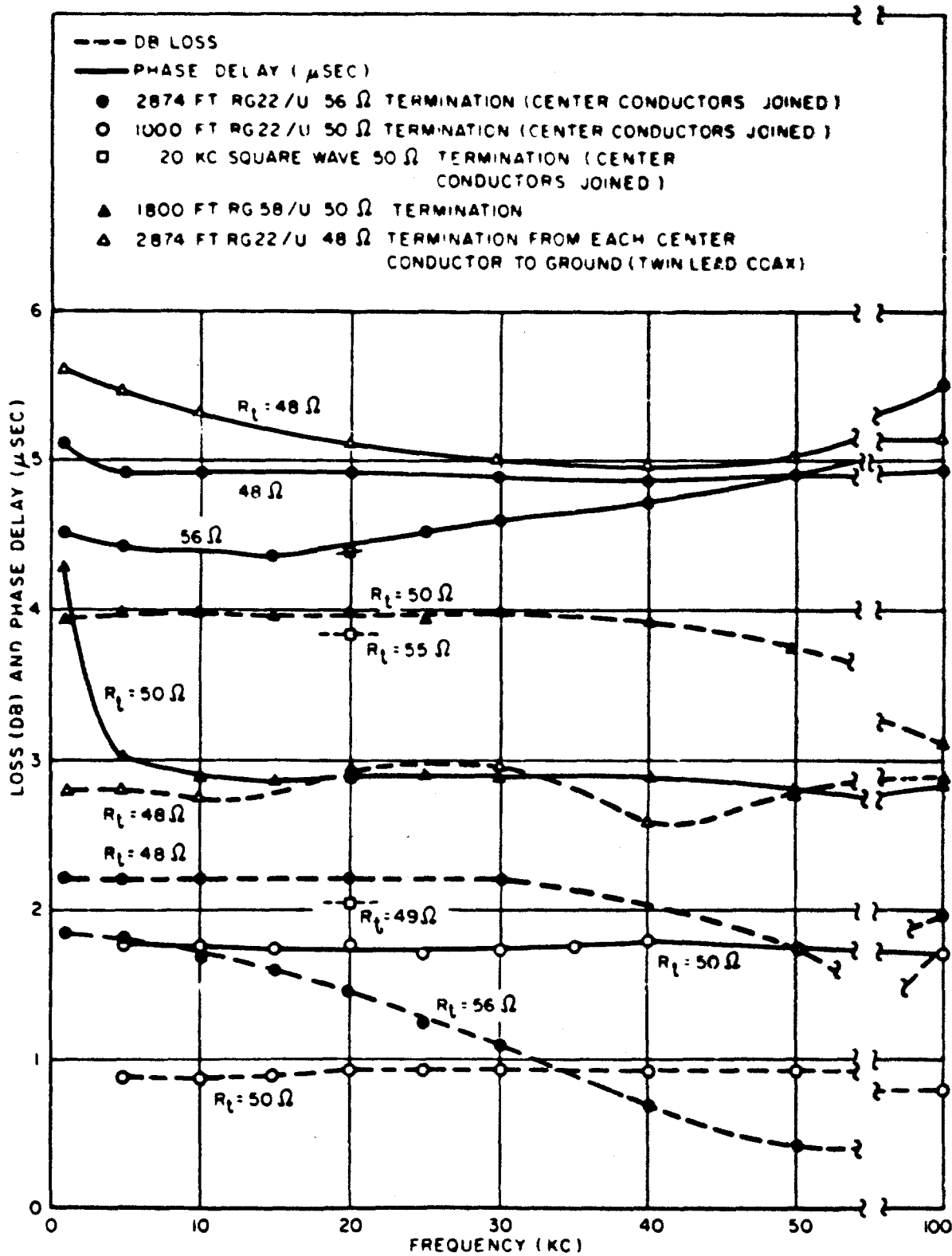


FIGURE 27. Loss and Phase Delay Through Coaxial Cable

REFERENCES

1. E. W. Seeley, "The Two-Loop Superdirective End-Fire Antenna." Naval Ordnance Laboratory, Corona, Calif., 1 April 1962. (NOLC Report 562.)
2. E. W. Seeley, "The Three-Loop Superdirective Antenna." Naval Ordnance Laboratory, Corona, Calif., 1 May 1962. (NOLC Report 563.)
3. E. W. Seeley, "N-Loop VLF Superdirective Arrays." Naval Ordnance Laboratory, Corona, Calif., 1 April 1963. (NOLC Report 580.)
4. E. W. Seeley, "Coaxial Loop Superdirective Arrays." Foundational Research Projects, April-June 1963. Naval Ordnance Laboratory, Corona, Calif., 1 September 1963. (NAVWEPS Report 8158.)
5. D. A. Schriener, E. W. Seeley, and C. N. Perle, "The Use of Sferics as a Signal Source in the Measurement of Very-Low-Frequency Antenna Patterns." Naval Ordnance Laboratory, Corona, Calif., 1 July 1963. (NOLC Report 581.)
6. A. G. Jean, H. E. Taggart, and J. R. Wait, "Calibration of Loop Antennas at VLF," J. Research Natl. Bur. Standards, C. Engr. and Instrumentation, Vol. 65, No. 3 (July-September 1961), pp. 189-193.

INITIAL DISTRIBUTION

	<u>Copies</u>		<u>Copies</u>
Chief, Office of Naval Research Navy Department Washington, D. C. 20360 Attn: Code 402C 418	1 2	Commander Naval Air Test Center Weapons Systems Test Division Patuxent River, Md. 20670 Attn: Code 32 323	1 1
Chief of Naval Operations Navy Department Washington, D. C. 20350 Attn: Code Op-723E Op-07TE	1 1	Commanding Officer and Director Navy Electronics Laboratory San Diego, Calif. 92152 Attn: Library	1 1
Chief, Bureau of Naval Weapons Navy Department Washington, D. C. 20360 Attn: Code R-3 R-12 RMGA-81, Jim Lee RTOS DLI-31	1 1 1 1 2	Commander Naval Missile Center Point Mugu, Calif. 93041 Attn: Code N03022 Commander Pacific Missile Range Point Mugu, Calif. 93041 Attn: Code 3215	1 1 1
Chief, Bureau of Ships Navy Department Washington, D. C. 20360 Attn: Code 362A	1	Commanding Officer Office of Naval Research Branch Office Box 39, Navy #100 Fleet Post Office New York, N. Y. 09501	1
Director Naval Research Laboratory Washington, D. C. 20390 Attn: Code 5320, J. M. Headrick 2027	1 1	Headquarters, North American Air Defense Command Ent Air Force Base Colorado Springs 12, Colo. Attn: NELC-AP	1
Director, Special Projects Navy Department Washington, D. C. 20360 Attn: Code SP-204 SP-2041	1 1	Naval Weapons Services Office Naval Base Philadelphia, Pa. 19112	2

	<u>Copies</u>		<u>Copies</u>
Headquarters Rome Air Development Center Air Force Systems Command, USAF Griffiss Air Force Base, N. Y. Attn: RAUEL-3, G. R. Weatherup		Defense Documentation Center Bldg. #5, Cameron Station Alexandria, Va. 22314	20
Commanding Officer Naval Ordnance Test Unit Atlantic Missile Range Patrick Air Force Base, Fla. Attn: SPP002		Director 1 Advanced Research Projects Agency Washington, D. C. 20390 Attn: Alvin Van Every	1
Foreign Technology Division Wright-Patterson Air Force Base, Ohio 45433 Attn: TDEED, W. L. Picklesimer TDATA, G. A. Long, Jr. TDCE, M. S. J. Graebner		1 National Bureau of Standards Boulder Laboratories Boulder, Colo. Attn: L. H. Tveten, 85.20	1
Headquarters, Air Force Cambridge Research Laboratories Laurence G. Hanscom Field Bedford, Mass. Attn: Dr. G. J. Gassman (CRUP) W. F. Ring (CRUI)		Director National Security Agency Fort George G. Meade, Md. Attn: C3/TDL	1
Headquarters, U. S. Air Force Office of Assistant Chief of Staff, Intelligence Policy & Programs Group, AFNINC Washington 25, D. C.		1 Director Weapons Systems Evaluation Group Office of the Director of Defense Research and Engineering Washington 25, D. C.	
Commanding Officer U. S. Army Materiel Command Washington 25, D. C. Attn: AMCRD-D		1 Electronic Defense Laboratories P. O. Box 205 Mountain View, Calif.	1
Commanding Officer Army Munitions Command Picatinny Arsenal Dover, N. J. 07801 Attn: SMUPA-VA6		1 Rensselaer Polytechnic Institute Plasma Research Laboratory Troy, N. Y. Attn: E. H. Holt, Director	1
		1 Dr. J. V. Harrington, Director Center for Space Research Massachusetts Institute of Technology Bldg. 33-109 Cambridge, Mass.	1

	<u>Copies</u>		<u>Copies</u>
Aero Geo Astro Corporation 13624 Magnolia Avenue Corona, Calif. 91720 Attn: A. W. Walters	1	Radio Corporation of America Aerospace Communications and Controls Division Burlington, Mass. Attn: J. Rubinovitz	1
Astrophysics Research Corporation 2444 Wilshire Blvd., Rm 512 Santa Monica, Calif. Attn: Dr. Alfred Reifman	1	The RAND Corporation 1700 Main Street Santa Monica, Calif. Attn: Library	1
Electro-Physics Laboratories ACF Electronics Division 3355 Fifty-Second Avenue Hyattsville, Md. Attn: W. T. Whelan	1	Raytheon Company Box 155 1415 Boston-Providence Turnpike Norwood, Mass. Attn: L. C. Edwards	1
General Electric Company Heavy Military Electronics Dept. Syracuse, N. Y. 13201 Attn: G. R. Nelson	1	Stanford Research Institute Menlo Park, Calif. Attn: R. Vincent L. T. Dolphin, Jr.	1 1
HRB Singer, Inc. Science Park P. O. Box 60 State College, Pa. Attn: E. J. Oelbermann	1	Stanford Research Institute Data Center c/o Communication Group Building 308B Menlo Park, Calif.	1
Massachusetts Institute of Technology Lincoln Laboratory Lexington 73, Mass. Attn: Dr. J. H. Chisholm	1	University of California Department of Mathematics Berkeley 4, Calif. Attn: Dr. E. J. Pinney	1
Institute of Science & Technology The University of Michigan P. O. Box 618 Ann Arbor, Mich. Attn: BAMIRAC Library	1	University of New Mexico Dept. of Electrical Engineering Albuquerque, N. Mex. Attn: R. H. Williams	1
Pickard and Burns, Inc. 103 Fourth Avenue Waltham 54, Mass. Attn: Dr. J. C. Williams, Research Dept.	1	Westinghouse Electric Corporation Air Arm Division Box 746 Baltimore, Md. 21203 Attn: David Fales	1

	<u>Copies</u>
NOLC:	
C. J. Humphreys, Code 40	1
F. C. Essig, Code 45	1
E. W. Seeley, Code 452	10
Technical Library, Code 234	2

**This Document Contains Page/s
Reproduced From
Best Available Copy**

NOLC 10-64-130

CONFIDENTIAL

Accession No. AD 20438

Harry Diamond Laboratories, Washington, D. C.
THE FLUERIC SCREAMER - Carl J. Campagnuolo, Allen B. Holmes

Fluorics
Noise-maker
Screamer
Acoustics

TM-67-19, November 1967, 10 pp text, 17 illus,
DA-1P014501A33B, AMCMS Code: 5011.11.71200
HDL Proj. No. 41100, CONFIDENTIAL Report

(C) Two fluoric screamers were developed at HDL to fulfill a request from the Southeast Asia theatre for a noise-making device that could be attached to the 2.75-in. rocket and the 105-mm howitzer projectile. Each of these devices is basically a ram-air-actuated fluoric oscillator with no moving parts. The purpose is to convert portions of the projectile kinetic energy into acoustical energy and to transmit the resulting sound to the ground.

(C) The device for the 105-mm projectile operates primarily in the subsonic range. A different design is required for the 2.75-in. rocket as it flies at supersonic velocities throughout its range. In simulated flight tests, at 2 kHz, sound pressure levels were indicated in excess of 135 dB (re 0.0002 dynes/cm²) at 25 ft from the device. Effective results were obtained in flight tests at the HDL Test Area and Aberdeen Proving Ground.

CONFIDENTIAL

CONFIDENTIAL

Accession No. AD 20438

Harry Diamond Laboratories, Washington, D. C.
THE FLUERIC SCREAMER - Carl J. Campagnuolo, Allen B. Holmes

Fluorics
Noise-maker
Screamer
Acoustics

TM-67-19, November 1967, 10 pp text, 17 illus,
DA-1P014501A33B, AMCMS Code: 5011.11.71200
HDL Proj. No. 41100, CONFIDENTIAL Report

(C) Two fluoric screamers were developed at HDL to fulfill a request from the Southeast Asia theatre for a noise-making device that could be attached to the 2.75-in. rocket and the 105-mm howitzer projectile. Each of these devices is basically a ram-air-actuated fluoric oscillator with no moving parts. The purpose is to convert portions of the projectile kinetic energy into acoustical energy and to transmit the resulting sound to the ground.

(C) The device for the 105-mm projectile operates primarily in the subsonic range. A different design is required for the 2.75-in. rocket as it flies at supersonic velocities throughout its range. In simulated flight tests, at 2 kHz, sound pressure levels were indicated in excess of 135 dB (re 0.0002 dynes/cm²) at 25 ft from the device. Effective results were obtained in flight tests at the HDL Test Area and Aberdeen Proving Ground.

CONFIDENTIAL

CONFIDENTIAL

Accession No. AD 20438

Harry Diamond Laboratories, Washington, D. C.
THE FLUERIC SCREAMER - Carl J. Campagnuolo, Allen B. Holmes

Fluorics
Noise-maker
Screamer
Acoustics

TM-67-19, November 1967, 10 pp text, 17 illus,
DA-1P014501A33B, AMCMS Code: 5011.11.71200
HDL Proj. No. 41100, CONFIDENTIAL Report

(C) Two fluoric screamers were developed at HDL to fulfill a request from the Southeast Asia theatre for a noise-making device that could be attached to the 2.75-in. rocket and the 105-mm howitzer projectile. Each of these devices is basically a ram-air-actuated fluoric oscillator with no moving parts. The purpose is to convert portions of the projectile kinetic energy into acoustical energy and to transmit the resulting sound to the ground.

(C) The device for the 105-mm projectile operates primarily in the subsonic range. A different design is required for the 2.75-in. rocket as it flies at supersonic velocities throughout its range. In simulated flight tests, at 2 kHz, sound pressure levels were indicated in excess of 135 dB (re 0.0002 dynes/cm²) at 25 ft from the device. Effective results were obtained in flight tests at the HDL Test Area and Aberdeen Proving Ground.

CONFIDENTIAL

CONFIDENTIAL

Accession No. AD 20438

Harry Diamond Laboratories, Washington, D. C.
THE FLUERIC SCREAMER - Carl J. Campagnuolo, Allen B. Holmes

Fluorics
Noise-maker
Screamer
Acoustics

TM-67-19, November 1967, 10 pp text, 17 illus,
DA-1P014501A33B, AMCMS Code: 5011.11.71200
HDL Proj. No. 41100, CONFIDENTIAL Report

(C) Two fluoric screamers were developed at HDL to fulfill a request from the Southeast Asia theatre for a noise-making device that could be attached to the 2.75-in. rocket and the 105-mm howitzer projectile. Each of these devices is basically a ram-air-actuated fluoric oscillator with no moving parts. The purpose is to convert portions of the projectile kinetic energy into acoustical energy and to transmit the resulting sound to the ground.

(C) The device for the 105-mm projectile operates primarily in the subsonic range. A different design is required for the 2.75-in. rocket as it flies at supersonic velocities throughout its range. In simulated flight tests, at 2 kHz, sound pressure levels were indicated in excess of 135 dB (re 0.0002 dynes/cm²) at 25 ft from the device. Effective results were obtained in flight tests at the HDL Test Area and Aberdeen Proving Ground.

CONFIDENTIAL

REMOVAL OF EACH CARD WILL BE NOTED ON INSIDE BACK COVER, AND REMOVED CARDS WILL BE TREATED AS REQUIRED BY THEIR SECURITY CLASSIFICATION.

This Document Contains Page/s
Reproduced From
Best Available Copy